NISTIR 5288

## Electronics and Electrical Engineering Laboratory

# Technical Progress Bulletin

J. M. Rohrbaugh
Compiler

November 1993

Covering Laboratory Programs,
July to September 1993
with 1994 EEEL Events Calendar

# 93-3

U.S. DEPARTMENT OF COMMERCE
Technology Administration
National Institute of Standards
and Technology
Electronics and Electrical
Engineering Laboratory
Semiconductor Electronics Division
Gaithersburg, MD 20899

NIST

NISTIR 5288

# Electronics and Electrical Engineering Laboratory

J. M. Rohrbaugh
Compiler

**U.S. DEPARTMENT OF COMMERCE**
Technology Administration
National Institute of Standards
and Technology
Electronics and Electrical
Engineering Laboratory
Semiconductor Electronics Division
Gaithersburg, MD 20899

# Technical Progress Bulletin

November 1993

Covering Laboratory Programs,
July to September 1993
with 1994 EEEL Events Calendar

# 93-3


**U.S. DEPARTMENT OF COMMERCE**
Ronald H. Brown, Secretary

UNDER SECRETARY FOR
TECHNOLOGY
Mary L. Good

NATIONAL INSTITUTE OF STANDARDS
AND TECHNOLOGY
Arati Prabhakar, Director

# ELECTRONICS AND ELECTRICAL ENGINEERING LABORATORY
# TECHNICAL PROGRESS BULLETIN, NOVEMBER 1993 ISSUE

## INTRODUCTION

This is the forty-fourth issue of a quarterly publication providing information on the technical work of the National Institute of Standards and Technology Electronics and Electrical Engineering Laboratory (EEEL). This issue of the EEEL Technical Progress Bulletin covers the third quarter of calendar year 1993.

Organization of Bulletin: This issue contains abstracts for all relevant papers released for publication by NIST in the quarter and citations and abstracts for such papers published in the quarter. Entries are arranged by technical topic as identified in the Table of Contents and alphabetically by first author under each subheading within each topic. Unpublished papers appear under the subheading "Released for Publication." This does not imply acceptance by any outside organization. Papers published in the quarter appear under the subheading "Recently Published." Following each abstract is the name and telephone number of the individual to contact for more information on the topic (usually the first author). This issue also includes a calendar of Laboratory conferences and workshops planned for calendar year 1994 and a list of sponsors of the work.

Electronics and Electrical Engineering Laboratory: EEEL programs provide national reference standards, measurement methods, supporting theory and data, and traceability to national standards. The metrological products of these programs aid economic growth by promoting equity and efficiency in the marketplace, by removing metrological barriers to improved productivity and innovation, by increasing U.S. competitiveness in international markets through facilitation of compliance with international agreements, and by providing technical bases for the development of voluntary standards for domestic and international trade. These metrological products also aid in the development of rational regulatory policy and promote efficient functioning of technical programs of the Government.

The work of the Laboratory is conducted by four technical research Divisions: the Semiconductor Electronics and the Electricity Divisions in Gaithersburg, Md., and the Electromagnetic Fields and Electromagnetic Technology Divisions in Boulder, Colo. In 1991, the Office of Law Enforcement Standards, formerly the Law Enforcement Standards Laboratory, was transferred to EEEL. This Office conducts research and provides technical services to the U.S. Department of Justice and State and local governments, and other agencies in support of law enforcement activities. In addition, the Office of Microelectronics Programs (OMP) was established in EEEL to coordinate the growing number of semiconductor-related research activities at NIST. Reports of work funded through the OMP are included under the heading "Semiconductor Microelectronics."

Key contacts in the Laboratory are given on the inside back cover; readers are encouraged to contact any of these individuals for further information. To request a subscription or for more information on the Bulletin, write to EEEL Technical Progress Bulletin, National Institute of Standards and Technology, Metrology Building, Room B-358, Gaithersburg, MD 20899 or call (301) 975-2220.

Laboratory Sponsors: The Laboratory Programs are sponsored by the National Institute of Standards and Technology and a number of other organizations, in both the Federal and private sectors; these are identified on page 41.

Note on Publication Lists: Publication lists covering the work of each division are guides to earlier as well as recent work. These lists are revised and reissued on an approximately annual basis and are available from the originating division. The current set is identified in the Additional Information section, page 37.

---

Certain commercial equipment, instruments, or materials are identified in this paper in order to specify adequately the experimental procedures. Such identification does not imply recommendation or endorsement by the National Institute of Standards and Technology, nor does it imply that the materials or equipment identified are necessarily the best available for the purpose.

TABLE OF CONTENTS

## FUNDAMENTAL ELECTRICAL MEASUREMENTS

Released for Publication

Early, E.A., and Clark, A.F., **The ac Josephson Effect in Parallel Junction Arrays**.

A general model of any arbitrary number of Josephson junction in a parallel array is presented, in which the junctions are described by the RSJ model and inductances, magnetic fields, and junction parameters are included. The differential equations which describe this model are derived. Current-voltage curves obtained from numerical solutions of these equations have, in addition to the usual integral Shapiro steps resulting from the ac Josephson effect, half-integral steps. Extensive simulations of the dependence of the step widths on ac current amplitude for two and three junctions in parallel show a variety of behaviors for both the integral and half-integral steps. Selected results are used in the following companion paper to verify our proposal that half-integral steps in high-$T_c$ grain-boundary junctions are a manifestation of a parallel array of junctions. Some results for the time dependence of various physical quantities are also presented.
[Edward A. Early, (301) 975-4228]

Early, E.A., Steiner, R.L., Clark, A.F., and Char, K., **Evidence For Parallel Junctions Within High-$T_c$ Grain-Boundary Junctions**.

Novel half-integral constant voltage steps were observed in many high-$T_c$ grain-boundary Josephson junctions of $YBa_2Cu_3O_{7-\delta}$ when a microwave field was applied. Five distinct observed behaviors of the widths of both integral and half-integral steps as a function of microwave amplitude, $\Delta I_{dc}(I_{ac})$, are reproduced by simulations of two or three junctions in parallel using the model presented in the preceding companion paper. This provides quantitative evidence that a single high-$T_c$ grain-boundary junction is composed of several junctions in parallel. These junctions are formed by the overlap of superconducting filaments on either side of the grain boundary. The spacing between junctions with large critical currents is $\sim 20\ \mu m$.
[Contact: Edward A. Early, (301) 975-4228]

Steiner, R.L., Early, E.A., and Clark, A.F., **Half-Integer Steps in Josephson Array Standards**, to be published in the Proceedings of the National Conference of Standards and Laboratories 1993 Workshop and Symposium, Albuquerque, New Mexico, July 25-29, 1993.

There is recently recorded evidence that the 10-V Josephson array voltage standard device used in research operations at NIST in Gaithersburg produces voltages at half-integer step values. These unusual steps occur intermittently, sometimes several times within a daily measurement workload of 20-reference outputs (approximately 100-step selections). A Josephson junction can produce half-integer steps by acting as two junctions in parallel, but they are unexpected in array voltage standards, although several other laboratories have also witnessed such steps in these devices. Their cause here could be a symptom of deterioration for this particular five-year-old device, or they could be related to the recent introduction of a new, higher power microwave source, and, thus, a potential problem for other array voltage systems. Methods for recognizing half-integer steps, programmed precautions added to continue automated operation, and possible adverse effects on daily operations are discussed.
[Contact: Richard L. Steiner, (301) 975-4226]

## FUNDAMENTAL ELECTRICAL MEASUREMENTS

Recently Published

Cage, M.E., **Dependence of Quantized Hall Effect Breakdown Voltage on Magnetic Field and Current**, Journal of Research of the National Institute of Standards and Technology, Vol. 98, No. 3, pp. 361-373 (1993).

When large currents are passed through a high-quality quantized Hall resistance device, the voltage drop along the device is observed to assume discrete, quantized states if the voltage is plotted versus the magnetic field. These quantized dissipative voltage states are interpreted as occurring when electrons are excited to higher Landau levels and then return to the original Landau level. The quantization is found to be, in general, both a function of magnetic field and current. Consequently, it can be more difficult to verify and determine dissipative voltage quantization

than previously suspected.
[Contact: Marvin E. Cage, (301) 975-4249]

Cage M.E., **Quantized Dissipation of the Quantum Hall Effect at High Currents**, IEEE Transactions on Instrumentation and Measurement, Vol. 42, No. 2, pp. 176-178 (April 1993).

Quantized dissipative voltage states are observed when large currents are passed through a high-quality quantized Hall resistance device. These dissipative states are interpreted as occurring when electrons are excited to higher Landau levels and then returned to the original Landau level. We show that the quantization is more complicated than previously thought. For example, the quantization can be a function of magnetic field. Therefore, the dissipative voltage quantization can, in general, be difficult to verify and determine.
[Contact: Marvin E. Cage, (301) 975-4224]

Early, E.A., Clark, A.F., Steiner, R.L., and Char, K., **Fractional Constant Voltage Steps in Parallel Arrays of Josephson Junctions**, American Physical Society Meeting Digest, Seattle, Washington, March 22-26, 1993, p. 836.

In single Josephson junctions, the ac Josephson effect produces integrally quantized constant voltage steps. With junctions in parallel, additional fractional constant voltage steps can also be present. We have extended the model of a previous study to include the effects of various parameters, such as the number of junctions, their inductances, and the normalized frequency, on the dependence of these constant voltage steps on magnetic field and microwave power. We have observed fractional steps in certain bi-epitaxial grain boundary high-$T_c$ junctions, and an extensive comparison of the results of simulations with experimental results indicate that these grain boundary junctions are composed of multiple junctions in parallel.
[Contact: Edward A. Early, (301) 975-4228]

Early, E.A., Steiner, R.L., Clark, A.F., and Char, K., **Half-Integral Constant Voltage Steps in Grain-Boundary High-$T_c$ Junctions**, Extended Abstracts of the Materials Research Society 1993 Spring Meeting, San Francisco, California, April 12-16, 1993, p. 388.

Some bi-epitaxial $YBa_2Cu_3O_{7-\delta}$ single grain boundary junctions have constant voltage steps at exactly half the voltages of the usual Shapiro steps resulting from the ac Josephson effect. The voltages of these additional steps are exactly half those of the Shapiro steps. These steps are termed half-integral. We have investigated the magnetic field dependence of the critical currents of these junctions as well as the relationship of the magnetic field and the individual junction parameters with the occurrence of the half-integral steps and their microwave power dependence. Extensive comparisons of our results with previous results and with simulations indicate that these grain boundary junctions are composed of multiple junctions in parallel.
[Contact: Edward E. Early, (301) 975-4228]

Eiles, T.M., Martinis, J.M., and Devoret, M.H., **Even-Odd Asymmetry of a Superconductor Revealed by the Coulomb Blockade of Andreev Reflection**, Physical Review Letters, Vol. 70, No. 12, pp. 1862-1865 (March 22, 1993).

We have measured at low temperatures the current through a submicrometer superconducting island connected to two normal metal leads by ultrasmall tunnel junctions. As the bias voltage is lowered well below twice the superconducting energy gap, the current changes from being *e* periodic with gate charge to 2*e* periodic. This behavior is clear evidence that there is a difference in the total energy between the ground states of an even and odd number of electrons on the island. The 2*e*-periodic current peaks are the first observation of the Coulomb blockade of Andreev reflection.
[Contact: Travis M. Eiles, (303) 497-3969]

Ghosh, R.N., and Williams, E.R., **Precision Capacitance Bridge Using a Single Electron Tunneling Electrometer**, American Physical Society Meeting Digest, Seattle, Washington, March 22-26, 1993, p. 697.

The charge of the electron can be determined by placing a known number of electrons on a calibrated capacitor and measuring the voltage drop across the capacitor. Recent developments in single-electron tunneling (SET) have shown how to

fabricate an electrometer with sufficient charge sensitivity ($10^{-4}$ e/√Hz at 10 Hz) to measure the charge. We report on a cryogenic capacitance bridge experiment using a SET electrometer to determine the capacitance ratio of two fused silica capacitors in a dilution refrigerator. We investigate questions of fundamental importance for the experiment to measure e, such as 1) the leakage rate of a capacitor at cryogenic temperatures, 2) the optimum circuit parameters for coupling the electrometer to the capacitance bridge while maintaining the electrometer sensitivity, 3) methods to minimize stray capacitance, and 4) techniques to reduce charge noise.
[Contact: Ruby N. Ghosh, (301) 975-4150]

Kautz, R.L., Zimmerli, G., and Martinis, J.M., **Self-Heating in the Coulomb-Blockade Electrometer**, Journal of Applied Physics, Vol. 73, No. 5, pp. 2386-2396 (March 1, 1993).

A detailed comparison between theory and experiment is used to demonstrate the presence of self-heating in the Coulomb-blockade electrometer. When three different heating models are considered, the best fit with experimental electrometer characteristics is obtained for a model in which the electron temperature of the island electrode is determined by heat transfer to the lattice via electron-phonon coupling. In the successful model, the temperature $T_i$ of the island electrons is related to the power $P_i$ dissipated in the island and the temperature $T_l$ of the phonons by $P_i = \Sigma\Omega(T_i^5 - T_l^5)$, where $\Sigma$ is an electron-phonon coupling parameter characteristic of the island material and $\Omega$ is the volume of the island. The best fit between theory and experiment yields a value of $\Sigma = 0.2$ nW/K$^5$/$\mu$m$^3$ for the electron-phonon coupling in aluminum. Our calculations show that the electron temperature of the island commonly exceeds 100 mK even when the lattice remains at 35 mK.
[Contact: Richard L. Kautz, (303) 497-3391]

Tew, W.L., and Williams, E.R., **A Flux Locked Current Source Reference**, Conference Record of the Conference on Precision Electromagnetic Measurements (CPEM '92), Paris, France, June 9-12, 1992, pp. 186-190.

The quantization of flux in a closed superconducting circuit is used to provide a stable reference current. A 10-mA current source is coupled via a toroidal transformer to a dc SQUID input and the resulting signal fed back as an error current. The result is a net current that exhibits stability of $1 \times 10^{-9}$ per hour and is quantized with a step size of 59.4 nA. This current is passed through a precision 100-Ω resistor and compared against zener diode references. The observed temperature coefficient for the flux transformer is 28.5 ± 2 parts per million/K at 4.2 K. Possible sources for the temperature dependence are discussed.
[Contact: Edwin R. Williams, (301) 975-6555]

Van Degrift, C.T., Yoshihiro, K., Palm, E.C., Wakabayashi, J., and Kawaji, S., **Re-Examination of Quantum Hall Plateaus**, IEEE Transactions on Instrumentation and Measurement, Vol. 42, No. 2, pp. 562-567 (April 1993). [Also published in the Conference Record of the Conference on Precision Electromagnetic Measurements (CPEM '92), Paris, France, June 9-12, 1992, pp. 288-289.]

Even though the practical unit of electrical resistance was tied to the quantum Hall effect in 1990, our understanding of the fundamental physics of current flow, contacting, and impurity effects in quantum Hall systems remains incomplete. This paper examines some recently discovered effects which may affect quantum Hall resistance determinations. We also describe improvements to the NIST potentiometric measurement system and present new data comparing the $i = 4$ plateaus of a Si-MOSFET nad a GaAs heterostructure with a room temperature reference resistance.
[Contact: Craig T. Van Degrift, (301) 975-4248]

## SEMICONDUCTOR MICROELECTRONICS

### Silicon Materials

Released for Publication

Lee, J.D., Park, J.C., Venables, D., Krause, S.J., and Roitman, P., **Stacking Fault Pyramid Formation and Energetics in Silicon-on-Insulator Material Formed by Cycles**.

The defect microstructure of silicon-on-insulator wafers produced by multiple oxygen implantation

and annealing was studied with transmission electron microscopy. The dominant defects are stacking fault pyramids (SFPs) located at the upper buried oxide interface at a density of $\sim 10^6$ $cm^{-2}$. The defects are produced by the expansion and interaction of narrow stacking fault (NSF) ribbons pinned to residual precipitates in the top silicon layer. Consideration of the energetics of the transformation from a collection of four NSF ribbons to a single SFP indicates that the reaction is energetically favorable below a critical NSF length. Thus, small defects are stable as SFPs while large defects are stable as NSF ribbons.
[Contact: Peter Roitman, (301) 975-2077]

Silicon Materials

Recently Published

Bullis, W.M., **Semiconductor Measurement Technology: Evolution of Silicon Materials Characterization: Lessons Learned for Improved Manufacturing**, NIST Special Publication 400-92 (July 1993).

The growth of the silicon device and integrated circuit industry has been closely coupled with the development of materials characterization technology. This paper traces this development from the beginning, when the industry was young and each manufacturer had to grow its own materials, develop its processes, assemble its measurement systems from component instruments, and fabricate its processing equipment, to the present, when a complex infrastructure support the industry. It also describes examples of both successful and unsuccessful developments in connection with other electronic materials. The critical factors in the widespread standardization and application of silicon characterization technology are: shared results and common goals among industry, government, and universities; an efficient mechanism for development of consensus standards with adequate expertise; standardization of parameters needed for orderly flow of materials in manufacturing together with standardized terminology, test methods, and formats to support detailed purchase specifications; and refinement of the measurement technology as the industry develops and becomes more sophisticated. Finally, a good methodology for process diagnosis and control is an essential feature for applying test procedures to the manufacturing environment. The successes and failures which occurred during the course of developing metrology tools for silicon can provide some insights into similar developments for the special needs of other electronic materials. In addition, many of the test procedures and standards developed for silicon materials and supporting technologies can be applied directly.
[Contact: David G. Seiler, (301) 975-2074]

Mayo, S., Lowney, J.R., and Roitman, P., **Characterization of Interface Defects in SIMOX Films**, Journal of Electronic Materials, Vol. 22, No. 2, pp. 207-214 (1993).

Defects in ungated n- or p-type and gated p-type resistors have been characterized by photoinduced transient spectroscopy (PITS). These resistors were fabricated with p-type separation by implanted oxygen (SIMOX) wafers with a single-energy 200-keV oxygen implant to a total fluence of $1.8 \times 10^{18}$ $cm^{-2}$. One wafer, used for gated resistor fabrication, was implanted at 595 °C and sequentially annealed at 1325 °C for 4 h in argon (plus 0.5 percent oxygen), followed by 4 h in nitrogen (plus 0.5 percent oxygen). Another wafer, used for ungated resistor fabrication, was implanted at 650 °C and annealed at 1275 °C for 2 h in nitrogen (plus 0.5 percent oxygen). The photoconductive response of these resistors to a 1-$\mu$s-long visible light pulse, measured at temperatures in the 80- to 170-K range, shows persistent photoconductive effects due to trapped minority carriers that are somewhat linked to the thermal anneal given to the SIMOX wafers. Our results indicate that more damage is present in the wafer annealed at 1275 °C than in the one annealed at 1325 °C. We model the photoconductive response in terms of a perpendicular built-in field created in the conductive film by trapped charge located at or near the interface with the buried oxide. Defects distributed throughout the conductive film body or located at the interface with the gate oxide are not expected to contribute significantly to the PITS signature, because of the fabrication of the gate oxide with standard metal-oxide semiconductor technology. We estimate the average interface trap density at the back interface is in the $10^{11}$ $cm^{-2}$ range.
[Contact: Santos Mayo, (301) 975-2045]

Mayo, S., Suehle, J.S., and Roitman, P., **Breakdown Mechanism In Buried Oxide Films**, Journal of Applied Physics, Vol. 74, No. 6, pp. 4113-4120 (September 1993).

Charge injection leading to catastrophic breakdown has been used to study the dielectric properties of the buried oxide layer in silicon implanted with high-energy oxygen ions. Current-versus-gate bias, current-versus-time, and capacitance-versus-gate bias were used to characterize, at various temperatures, MOS capacitors with areas in the $1 \times 10^{-4}$ to $1 \times 10^{-2}$ $cm^2$ range fabricated with commercially available single- or triple-implant SIMOX (Separation by IMplanted OXygen) wafers. Our data show that injected charge accumulates in the buried oxide at donor-like oxide traps ultimately leading to catastrophic breakdown. We have identified both Poole-Frenkel and Fowler-Nordheim conduction as well as impact-ionization mechanisms in the oxide. The charge- and field-to-breakdown in the best buried oxides are, respectively, near 1 C $cm^{-2}$ and 10 MV $cm^{-1}$, similar to the thermally grown oxide parameters. Cumulative distributions of these parameters measured over large number of capacitors show that the frequency of breakdown events caused by extrinsic defects is scaled with the capacitor area. Intrinsic and extrinsic defect distributions are broader than with thermally grown oxides.
[Contact: Santos Mayo, (301) 975-2045]

Compound Materials

Recently Published

Lowney, J.R., Seiler, D.G., Thurber, W.R., Yu, Z., Song, X.N., and Littler, C.L., **Heavily Accumulated Surfaces of Mercury Cadmium Telluride Detectors: Theory and Experiment**, Journal of Electronic Materials, Vol. 22, No. 8, pp. 985-991 (1993).

Some processes used to passivate n-type mercury-cadmium-telluride photoconductive infrared detectors produce electron accumulation layers at the surfaces, which result in 2D electron gases. The dispersion relations for the electric subbands that occur in these layers have been calculated from first principles. Poisson's equation for the built-in potential and Schroedinger's equation for the eigenstates have been solved self-consistently. The cyclotron effective masses and Fermi energies have been computed for each subband density for 12 total densities between 0.1 to $5.0 \times 10^{12}$ $cm^{-2}$. The agreement with Shubnikov-de Haas measurements is very good at lower densities with possible improvement if band-gap narrowing effects were to be included. At higher densities, larger differences occur. The simple 2D description is shown to break down as the density increases because the wave functions of the conduction and valence bands cannot be well separated by the narrow band gap of long-wavelength detectors. These results provide a basis for characterizing the passivation processes, which greatly affect device performance.
[Contact: Jeremiah R. Lowney, (301) 975-2048]

Pellegrino, J.G., Qadri, S.B., Cotell, C.M., Amirtharaj, P.M., Nguyen, N.V., and Comas, J., **Interface Sharpness During the Initial Stages of Growth of Thin, Short-Period III-V Superlattices**, Journal of Vacuum Science and Technology A., Vol. 11, No. 4, pp. 917-922 (July/August 1993).

Superlattices composed of III-V heterostructures have established applications in high-speed electronic and optoelectronic devices. As layer thicknesses are reduced, the role of heterostructure interface sharpness becomes more critical to ensuring high-quality two-dimensional growth. In this work, short-period (less than 1-nm) superlattices with active layer thickness of 31 nm were investigated to assess interface roughness in the initial stages of growth. X-ray diffraction was used to evaluate interface roughness and to calculate superlattice periodicity. Results suggest that surface roughening by islanding may be promoted by GaAs buffer layers that are 10 nm to 100 nm thick. Smoother interfaces were obtained in samples with buffer layers 250 nm and greater.
[Contact: Joseph G. Pellegrino, (301) 975-2123]

Seiler, D.G., Mayo, S., and Lowney, J.R., **$Hg_{1-x}Cd_xTe$ Characterization Measurements: Current Practice and Future Needs**, Semiconductor Scientific Technology, Vol. 8, pp. 753-776 (1993).

An extensive industrial survey of the importance and use of characterization measurements for HgCdTe materials, processes, and devices has been com-

pleted. Seventy-two characterization/measurement techniques were considered, and thirty-five responses were received. This information was sought for a study on materials characterization and measurement techniques of parameters and properties necessary to improve the manufacturing capabilities of HgCdTe infrared detectors. The nature of materials characterization is defined, and an overview is given of how it is related to improving IR detector manufacturing. Finally, we present a description of the characterization survey and a summary of the survey results. Major aspects of the results include: (1) ranking the 72 techniques by their importance and frequency of use; (2) listing the parameters or properties determined by each technique; (3) enumerating the most important properties needed to be measured; (4) indicating key measurement techniques that most need to be developed, enhanced, or improved; and (5) giving key overall comments.
[Contact: David G. Seiler, (301) 975-2081]

Steiner, B., Comas, J., Tseng, W.F., Laor, U., and Dobbyn, R.C., **Defects in III-V Materials and the Accommodation of Strain in Layered Semiconductors**, Journal of Electronic Materials, Vol. 22, No. 7, pp. 725-737 (August 1993).

High-resolution monochromatic synchrotron-radiation diffraction images of five, high-quality epitaxial heterojunctions on silicon, gallium-arsenide, and indium-phosphide substrates display several forms of accommodation to lattice mismatch. From the images, we deduce a coherent set of factors for the loss of crystalline order in layered semiconducting crystals. Lattice mismatch is demonstrated in each of the systems by warping after layer deposition. Nevertheless, local lattice orientation is maintained across each layer interface. In two of the systems, one severely mismatched while the other is not, no arrays of dislocations appear. Sets of mixed linear lattice mismatch dislocations, consistent with identification as 60° dislocations, are found in two of the other systems with intermediate degrees of mismatch. A set of pure edge dislocations penetrating all layers is found in a system with a grid structure. These observations indicate that the formation of extensive arrays of dislocations during uniform 1-$\mu$m-layer deposition depends not only on the extent of lattice mismatch and layer thickness, but also on the degree of crystalline order of the substrate. Establishment of a nonpseudomorphic layer mismatched with the substrate by several tenths of a percent is an important factor, as previously determined. However, localized absence of crystalline order, e.g., in the form of scratches or dislocations in the substrate, appears also to be required for the formation of arrays of interface mismatch dislocations. Where these criteria are not fulfilled, the formation of dislocations in uniform layered systems is inhibited. Localized residual stress can initiate dislocation formation even where it would not appear in uniform layers. The images show also that crystalline disorder in state-of-the-art indium phosphide differs markedly from that in comparable gallium arsenide. Understanding of crystalline order in both monolithic materials is extended by this work.
[Contact: James Comas, (301) 975-2061]

Vanzura, E.J., Weil, C.M., and Williams, D.F., **Complex Permittivity Measurements of Gallium-Arsenide Using a High-Precision Resonant Cavity**, Conference Record of the Conference on Precision Electromagnetic Measurements (CPEM '92), Paris, France, June 9-12, 1992, pp. 103-104.

Data are presented on the complex permittivity of gallium arsenide, as measured at room temperature in the 8- to 12-GHz frequency range. The measurements were performed using a mode-filtered cylindrical cavity resonator with helically wound walls. The estimated accuracies are $\pm$0.4% in relative permittivity and $\pm$5% in loss tangent at 10 GHz.
[Contact: Eric J. Vanzura, (303) 497-5752]

## Analysis and Characterization Techniques

### Recently Published

Albers, J., and Berkowitz, H.L., **Semiconductor Measurement Technology: A Collection of Computer Programs for Two-Probe Resistance (Spreading Resistance) and Four-Probe Resistance Calculations, RESPAC**, NIST Special Publication 400-91 (June 1993).

This report presents and describes a number of FORTRAN programs which may be used to perform two-probe resistance (spreading resistance) and four-probe resistance calculations for vertically

nonuniform resistivity structures. These programs fall into three general categories. They are: 1) programs for calculating the two-probe resistance (spreading resistance) from the resistivity profile, 2) programs for calculating the resistivity profile from the two-probe resistance (the inverse of 1), and 3) programs for calculating the four-probe resistance from the resistivity profile. Programs in the first and third category are useful for understanding the effects of resistivity variations on the two-probe resistance (spreading resistance) and the four-probe resistance. Programs in the second category are useful for extracting the resistivity profile from spreading resistance data (either measured or calculated). All of the programs are based upon the Schumann and Gardner solution of the multilayer Laplace equation. As such, local charge neutrality is assumed. The limitations of this assumption are described in the text. The first part of this report consists of an outline of the derivation of the Schumann and Gardner multilayer Laplace equations. In addition, there is a discussion of the evolution and simplification of this model which has taken place over the past two decades. This part of the report is intended to provide the reader with a background so as to make optimal use of the computer programs. Special attention is paid to the aspects which make the individual programs different from others in the same category. In addition, sample input data used in the programs and the corresponding output data calculated by the programs are also presented. The final parts of the report (the appendices) contain annotated, internally-documented listings of the FORTRAN source codes. In all, there are ten programs contained in the RESPAC package. The FORTRAN source code (total of about 123 kbytes) and sample input and output data files are available in ASCII format using a number of transfer vehicles. These include: standard 8-track magnetic tape (ASCII, density = 1600, record = 80, block = 1600), 5.25-in. (360 kbyte and 1.2 Mbyte) DOS-formatted floppy disks, and using electronic mail over the Internet. This package is self-contained and is straightforward to run once the FORTRAN is compiled and linked by the user supplied software. The sample input and output data files are included so that the user can check the programs for proper operation as well as to become acquainted with the setup and use of the codes.
[Contact: John Albers, (301) 975-2075]

Kim, J.S., Seiler, D.G., and Tseng, W.F., **Multicarrier Characterization Method for Extracting Mobilities and Carrier Densities of Semiconductors from Variable Magnetic Field Measurements**, Journal of Applied Physics, Vol. 73, No. 12, pp. 8324-8335 (June 15, 1993).

A simple, practical method is described to extract the carrier concentration and mobility of each component of a multicarrier semiconductor system (which may be either a homogeneous or multilayered structure) from variable magnetic field measurements. Advantages of the present method are mainly due to the inclusion of both the parallel- and transverse-components of the conductivity tensor and normalization of these quantities with respect to the zero-field parallel component of the conductivity tensor. This method also provides a simple, direct criterion by which one can easily determine whether the material under test is associated with a one-carrier or multicarrier conduction. The method is demonstrated for a simple one-carrier system (GaAs single-channel HEMT structure) and two multicarrier systems (an InGaAs-GaAs double-channel HEMT structure and two types of carriers present in an InGaAs single-channel HEMT structure). The analysis of the experimental data obtained on these specimens demonstrates the utility of the method presented here for extracting carrier concentrations and mobilities in advanced semiconductor structures.
[Contact: Jin S. Kim, (301) 975-2238]

## Device Physics and Modeling

### Recently Published

Hefner, A.R., and Blackburn, D.L., **Thermal Component Models for Electro-Thermal Network Simulation**, Proceedings of the Semiconductor Thermal Measurement and Management Symposium, Austin, Texas, February 2-4, 1993, pp. 88-96.

A procedure is given for developing thermal component models for electro-thermal network simulation. In the new electro-thermal network simulation methodology, the simulator solves for the temperature distribution within the semiconductor devices, packages, and heat sinks (thermal network) as well

as the currents and voltages within the electrical network. The thermal network is represented as an interconnection of compact thermal component models so that the system designer can readily interchange different thermal components and examine different configurations of the thermal network. To facilitate electro-thermal network design, the interconnection of the thermal component models is specified by the user in the same way as the interconnection of the electrical network components is specified. The thermal component models are also parameterized in terms of structural and material parameter so that the details of the heat transport physics are transparent to the user. Example electro-thermal network simulations are given, and the temperature measurement methods used to validate the thermal component models are described.
[Contact: Allen R. Hefner, (301) 975-2071]

Mantooth, H.A., and Hefner, A.R., **Electro-Thermal Simulation of an IGBT PWM Inverter**, Proceedings of the 1993 Power Electronics Specialists Conference, University of Seattle, Seattle, Washington, June 21, 1993, pp. 75-84.

A recently developed electro-thermal network simulation methodology is used to analyze the behavior of a full-bridge, pulse-width-modulated (PWM), voltage-source inverter which uses Insulated Gate Bipolar Transistors (IGBTs) as the switching devices. The electro-thermal simulations are performed using the Saber circuit simulator and include the control logic circuitry, the IGBT gate drivers, the physics-based IGBT electro-thermal model, and the thermal network component models for the power device silicon chips, packages, and heat sinks. It is shown that the thermal response of the silicon chip determines the IGBT temperature rise during the device switching cycle. The thermal response of the device TO247 package and silicon chip determines the device temperature rise during a single phase of the 60-Hz sinusoidal output. Also, the thermal response of the heat sink determines the device temperature rise during the system start-up and after load impedance changes. It is also shown that the full electro-thermal analysis is required to accurately describe the power losses and circuit efficiency.
[Contact: Allen R. Hefner, (301) 975-2071]

Insulators and Interfaces

Recently Published

Chandler-Horowitz, D., Nguyen, N.V., Marchiando, J.F., and Amirtharaj, P.M., **Metrologic Support for the DARPA/NRL-XRL Mask Program: Ellipsometric Analyses of SiC Thin Films on Si**, NISTIR 4860 (January 1993).

Ellipsometric analyses were performed on a number of amorphous SiC films grown on Si which are currently being considered for X-ray lithography (XRL) mask membranes. The analyses and conclusions increase the accuracy with which the layer thicknesses can be determined. In addition, materials-related information such as the presence of surface roughness, Si and graphite phases, as well as densification, can be discerned from the data. The sensitivity of ellipsometry to very small changes in the phase ($\leq 2 \times 10^{-3}$ deg) of light makes it an extremely accurate optical tool capable of detecting small changes in thickness or optical properties. Samples were measured by single-frequency and spectroscopic ellipsometry. The measurements were analyzed by using a number of models. Three models with increasing degree of complexity and sophistication for the amorphous SiC film are compared: an isotropic one-layer model, an isotropic two-layer model that accommodates a surface layer/region, and a uniaxial one-layer model to account for possible built-in strain in the film. The two-layer model was found to give the most consistent fit to the experimental data. Here, the second layer is believed to be a top layer of surface roughness about 4 to 5 nm thick. The omission of this second layer can adversely affect the determination of the sample optical parameters, including accurate thickness measurements.

Mattis, R.L., **MAESTRO: A Front-End to the MAIN1 Program for Multiple-Angle Measurement of Silicon Dioxide Layers**, NISTIR 4969 (December 1992).

MAESTRO is an interactive program which serves as a front-end to the MAIN1 computer program for processing ellipsometric data. It is applicable when MAIN1 is used to characterize silicon dioxide layers on silicon substrates using a single pair of Delta-psi values, using repeated pairs of Delta-psi values

taken at the same nominal angle of incidence, or using pairs of Delta-psi values taken at multiple angles of incidence. MAESTRO stands for Multiple-Angle Ellipsometry for Supplying Thickness and Refractive index Output. It consists of two FORTRAN programs and a VMS DCL command procedure. An implementation for MS-DOS is also available. MAESTRO is used to prepare the X.DAT file required by MAIN1 and to give this file and the MAIN1 output files user-defined names.
[Contact: Richard L. Mattis, (301) 975-2235]

Mattis, R.L., and Belzer, B.J., **STREMDA: A Front-End to the MAIN1 Program for Characterizing Standard Reference Silicon Dioxide Layers**, NISTIR 4925 (October 1992).

STREMDA is an interactive program which serves as a front-end to the MAIN1 computer program when that program is being used to characterize the silicon dioxide layers on silicon substrates which comprise NIST Standard Reference Material 2530 series. STREMDA stands for STandard REference Material Data Analysis. It consists of two FORTRAN programs and a VMS DCL command procedure. An implementation for MS-DOS is also available. STREMDA is used to prepare the X.DAT file required by MAIN1 and to give this file and the MAIN1 output files user-defined names.
[Contact: Richard L. Mattis, (301) 975-2235]

Nguyen, N.V., Pellegrino, J.G., Amirtharaj, P.M., Seiler, D.G., and Qadri, S.B., **Interface Roughness of Short-Period AlAs/GaAs Superlattices Studied by Spectroscopic Ellipsometry**, Journal of Applied Physics, Vol. 73, No. 11, pp. 7739-7746 (June 1, 1993).

Spectroscopic ellipsometry (SE) has been used to study the effects of interface roughness on the optical properties of ultrathin short-period 3 x 3 GaAs/AlAs superlattices grown by molecular-beam epitaxy (MBE). The complex dielectric function and thickness of the whole superlattice and the thickness of the native oxide overlayer were simultaneously determined by an inversion technique from data in the 1.5- to 5.0-eV region. The main optical critical points $E_0$, $E_0 + \Delta_0$, $E_1$, $E_1 + \Delta_1$, and $E_2$ were deduced by line-shape fitting of the second derivative of the complex dielectric function of the superlattice to the analytical line-shape expression. The interface roughness is found to shift the optical transitions, except $E_2$, to higher energy and broaden their line shapes. A simple interpretation of the shift and broadening is given. The interface roughness and layer thicknesses obtained by SE are found to be consistent with the results of x-ray diffraction and Raman scattering studies previously reported. The results in this study demonstrate the capability of the post-growth nondestructive characterization by SE to provide useful information about the interface quality of superlattice structures, and consequently to optimize the MBE growth conditions in order to achieve the desired structural parameters.
[Contact: Nhan Van Nguyen, (301) 975-2044]

## Dimensional Metrology

### Recently Published

Postek, M.T., Lowney, J.R., Vladar, A.E., Keery, W.J., Marx, E., and Larrabee, R.D., **X-Ray Mask Metrology: The Development of Linewidth Standards for X-Ray Lithography**, Proceedings of SPIE (The International Society for Optical Engineering, P.O. Box 10, Bellingham, Washington 98227-0010), Electron-Beam, X-Ray, and Ion-Beam Submicrometer Lithographies for Manufacturing III, Vol. 1924, pp. 435-449 (1993).

The calibration of masks used in X-ray lithography has been successfully accomplished in the scanning electron microscope (SEM) by utilizing the transmitted scanning electron detection technique. This has been made possible because these masks present a measurement subject different from most (if not all) other objects used in semiconductor processing because the support membrane is, by design, X-ray transparent. This characteristic can be used as an advantage in electron-beam-based mask metrology since, depending upon the incident electron beam energies, substrate composition, and substrate thickness, the membrane can also be essentially electron transparent. The areas of the mask where the absorber structures are located are essentially X-ray opaque as well as electron opaque. Viewing the sample from a perspective below an X-ray mask (by placing the detector beneath the mask) provides excellent electron signal contrast between the absorber structure and the base membrane. Thus, the mask can be viewed in the transmitted electron detection mode of the SEM and precise, potentially

accurate dimensional measurements can be made. Monte Carlo modeling of the transmitted electron signal was used to support this work in order to determine the optimum electron detector position and characteristics. One unique advantage afforded by the X-ray mask is that in the transmitted electron detection mode, the modeling of the electron beam/specimen interaction becomes far less difficult than in the modeling of typical secondary electron images of opaque objects. Many of the inelastically scattered beam electrons and the low-energy secondary electrons can be excluded from the detector and, therefore, do not need to be accurately modeled. The comparison between the theoretically modeled electron-beam interaction model data and actual experimental data was also made. The theoretical profiles were shown to agree extremely well, particularly with regard to the wall slope characteristics of the structure obtained from the SEM video profiles. Therefore, the theory can be used to identify the location of the edge of the absorber. This determination shows the way to standards development and a more precise edge location algorithm for measurement of this type of structure in commercial instrumentation. The transmitted electron detection mode is also useful in both mask inspection and mask repair, because the high contrast of the image allows rapid determination of mask defects and high-density particle detection as well as registration measurements. This work represents the potential for the first accurate linewidth measurement standard measured at NIST in the SEM as well as the potential for linewidth standards for the X-ray lithography community.
[Contact: Michael T. Postek, (301) 975-2299]

Integrated-Circuit Test Structures

Released for Publication

Allen, R.A., and Schuster, C.E., **An Electrical Test Structure for Improved Measurement of Feature Placement and Overlay in Integrated Circuit Fabrication Processes**, to be published in the Proceedings of the Government Microcircuit Applications Conference 1993, New Orleans, Louisiana, November 1-5, 1993.

The modified voltage-dividing potintiometer test structure, for electrical measurement of feature placement and overlay in IC fabrication processes, has recently been applied to several multi-step processes. We describe two applications, present our measurment results, and discuss validating the results.
[Contact: Richard A. Allen, (301) 975-5026]

Integrated-Circuit Test Structures

Recently Published

Cresswell, M.W., Allen, R.A., Linholm, L.W., Ellenwood, C.H., and Teague, E.C., **Test Structure for the In-Plane Locations of Projected Features with Nanometer-Level Accuracy Traceable to a Coordinate Measurement System**, Proceedings of the 1993 IEEE International Conference on Microelectronic Test Structures, Sitges, Barcelona, Spain, March 22-25, 1993, pp. 255-261.

A new test structure has been designed to measure the positions of the images of an array of fiducial marks projected from a mask into a resist film on a substrate. The resist film on the substrate covers a nominally matching array of partially formed versions of the test structure prepatterned in a conducting film. Instances of the finished structure are formed on the substrate by further selective removal of conducting material from the partially formed test structures where they are overlaid by images of the fiducial marks on the mask. At each array point, the feature of the completed test structure that is defined by the overlay of the image of the fiducial marks on the mask is called the pointer. The part of the partially formed test structure that is unaffected by the overlay of the images of the fiducial marks on the mask serves as a ruler. Electrical testing accurately provides the precise location of the pointer relative to the ruler within each test structure. This paper describes the test structure and provides examples of measurements that indicate precision to within less than 2 nm and accuracy of better than 7 nm.
[Contact: Michael W. Cresswell, (301) 975-2072]

Kopanski, J.J., and Schuster, C.E., **Review of Semiconductor Electronic Test Structures with Applications to Infrared Detector Materials and Processes**, Semiconductor Scientific Technology, Vol. 8, pp. 888-910 (July 1993).

The impact of electronic test structures, as they have been applied to silicon integrated circuits and gallium-arsenide monolithic-microwave integrated circuits, is reviewed. Principles for the use of test structures with possible applications to infrared (IR) detector technology based on HgCdTe and other materials are emphasized. The uses of test structures for Si and GaAs, test chip design methodology, and some examples of how test structures have been applied for process control and to increase yield are discussed. Specific test structures and techniques that have been applied to IR detectors are also reviewed. The basic design considerations and measurements possible with each class of test structure are discussed. The important experience of the Si and GaAs industries, applicable to IR detectors, is that significant yield improvement is possible with improved process control using test structures.
[Contact: Joseph J. Kopanski, (301) 975-2089]

Teague, E.C., Linholm, L.W., Cresswell, M.W., Penzes, W.B., Kramar, J.A., Scire, F.E., Villarrubia, J.S., and Jun, J.S., **Metrology Standards for Advanced Semiconductor Lithography Referenced to Atomic Spacings and Geometry**, Proceedings of the 1993 IEEE International Conference on Microelectronic Test Structures, Sitges, Barcelona, Spain, March 22-25, 1993, pp. 213-217.

This paper outlines how the needs for calibrating the positional accuracy of features on an X-ray mask membrane or an optical reticle can be addressed by application of a high-accuracy coordinate metrology system known as the NIST Molecular Measuring Machine (M-Cubed). Based on scanning tunneling microscopy and state-of-the-art heterodyne optical interferometry, the measurements of M-Cubed are referenced to fundamental standards of length and angle and with the atomic-resolution of its scanning tunneling microscope probe will be validated against the interatomic spacings and geometry of single-crystal surfaces. Thus, through the use of a stable reference grid, serving as an intermediate calibration artifact, the positional accuracy of features on an X-ray mask membrane or an optical reticle can be referenced to fundamental standards of length and angle by means of the metrology system of M-Cubed. The performance goal of M-Cubed is to achieve uncertainties of 1 nm or less for point-to-point distance measurement within a 50-mm x 50-mm area. In a companion paper, a new technique has been developed which combines the capabilities of an electrical test structure with the metrology system of M-Cubed to provide traceable dimensional measurements aimed at uncertainties less than 2 nm.
[Contact: Loren W. Linholm, (301) 975-2052]

Microfabrication Technology

Recently Published

Chang, J. Y-C., Abidi, A.A., and Gaitan, M., **Large Suspended Inductors on Silicon and Their Use in a CMOS RF Amplifier**, IEEE Electron Device Letters, Vol. 14, No. 5, pp. 246-248 (May 5, 1993).

Large spiral inductors on oxide over silicon are shown to operate beyond the UHF band when the capacitance and loss resistance are dramatically reduced by selective removal of the underlying substrate. Using a 100-nH inductor whose self-resonance lies at 3 GHz, a tuned amplifier with a gain of 14 dB centered at 770 MHz has been implemented in a standard digital 2-$\mu$m CMOS IC process. The core amplifier noise figure is 6 dB, and power dissipation 7 mW on a 3-V supply.
[Contact: Michael Gaitan, (301) 975-2070]

Christensen, D.H., Hill, J.R., Schaafsma, D.T., Hickernell, R.K., Pellegrino, J.G., and Tseng, W.F., **Vertical-Cavity Semiconductor Structures: Materials Characterization**, Proceedings of the Conference on Lasers and Electro-Optics, Baltimore, Maryland, May 2-7, 1993, pp. 234-235.

Materials characterization of a variety of vertical-cavity semiconductor structures is reported. Double-crystal X-ray diffractometry, reflectance spectroscopy, and photoluminescence measurements are correlated and used to determine cavity and Bragg mirror layer thicknesses.
[Contact: David H. Christensen, (303) 497-3354]

Dagata, J.A., and Tseng, W., **Ambient Scanning Tunneling Spectroscopy of *n*- and *p*-type Gallium Arsenide**, Applied Physics Letters, Vol. 62, No. 6, pp. 591-593 (February 8, 1993).

Ambient scanning tunneling spectroscopy (STS) of

*n*- and *p*-doped GaAs (110) and (100) surfaces, prepared with a stable, electrically transparent surface oxide, reveals that the current-voltage (*I-V*) characteristics of these surfaces are essentially identical to the *I-V* properties of the free (110) surface cleaved in ultrahigh vacuum. These results demonstrate for the first time that: (1) meaningful STS spectra of GaAs surfaces can be obtained *in air*, (2) the passivating layer, consisting of a stable, ultrathin oxide, allows the scanning tunneling microscopy tip to probe the bulk electrical properties of the semiconductor, and (3) quantitative doping information, $10^{15} < N_A, N_D < 10^{19}$ $cm^{-3}$, can be extracted from the STS data.
[Contact: Wen F. Tseng, (301) 975-5291]

Dagata, J.A., Tseng, W.F., and Silver, R.M., **Scanning Tunneling Microscopy of Passivated Gallium Arsenide under Ambient Conditions**, Journal of Vacuum Science Technology A, Vol. 11, No. 4, pp. 1070-1074 (July/August 1993).

Scanning tunnel spectroscopy of *n*- and *p*-type GaAs (110) and (100) surfaces, prepared with a novel electrically transparent surface oxide, reveals that the current-voltage (*I-V*) characteristics of these surfaces obtained in air exhibit transport properties typical of the bulk band structure, a result which was previously obtained only on (110) GaAs surfces cleaved in ultrahigh vacuum. The passivation technique has been used to obtain stable images of cleaved, molecular-beam-epitaxy-grown GaAs *pn* junctions in air as well. The results of this study demonstrate that quantitative doping information over the range of $10^{15} < N_A, N_D < 10^{19}$ $cm^{-3}$ can be extracted from scanning tunneling microscopy data on passivated GaAs surfaces under ambient conditions.
[Contact: Wen F. Tseng, (301) 975-5291]

Gaitan, M., Suehle, J.S., Kinard, J.R., and Huang, D.X., **Multijunction Thermal Converters by Commercial CMOS Fabrication**, Proceedings of the IEEE Instrumentation/Measurement Technology Conference, Irvine, California, May 18-20, 1993, pp. 243-244.

New multijunction thermal converters fabricated in a commercial CMOS foundry are described and the results of measurements of their ac-dc transfer characteristics are given.
[Contact: Michael Gaitan, (301) 975-2070]

Lee, K.C., **A Lithium-Drift Technique for Making Submicrometer Thick Silicon Membranes**, Proceedings of the Symposium on Electrochemical Microfabrication, Phoenix, Arizona, October 16, 1992, pp. 1-6 (1993).

An electrochemical method for preparing silicon membranes that relies on the use of room-temperature lithium diffusion to create a compensated, high-resistivity layer with very low etch rate near one surface of a p-type Si wafer is described. The bulk wafer can be dissolved away, leaving behind a membrane that can be between several tenths of micrometers and several micrometers in thickness. The various parameters that affect the thickness of the membrane are described. As an example of this technique, the preparation of a 670-nm-thick silicon membrane is described.
[Contact: Kevin C. Lee, (301) 975-4236]

Marshall, J.C., Parameswaran, M., Zaghloul, M.E., and Gaitan, M., **High-Level CAD Melds Micromachined Devices with Foundries**, IEEE Circuits and Devices, Vol. 8, No. 6, pp. 10-17 (November 1992).

The methodology for implementing the design of silicon micromachined devices in a standard CMOS foundry process is discussed, and a modified Magic technology file is introduced. The modified technology file is used to design silicon micromachined devices that are fabricated using a standard CMOS foundry through the MOSIS service. An additional maskless etch in EDP is required to realize the micromechanical structures once devices are delivered. The modified technology file implements a layer that we call "open" that consists of a combination of vias and contact cuts. This open area exposes the silicon surface for an anisotropic etch procedure that creates suspended bridges of polysilicon or metal encapsulated in $SiO_2$. Results from fabricated chips are included.
[Contact: Janet C. Marshall, (301) 975-2049]

Russek, S.E., Roshko, A., Sanders, S.C., Rudman, D.A., Ekin, J.W., and Moreland, J., **Growth of Laser Ablated $YBa_2Cu_3O_{7-\delta}$ Films as Examined by RHEED and Scanning Tunneling Microscopy**, Materials Research Society 1992 Fall Pro-

ceedings, Houston, Texas, November 30-December 4, 1992, pp. 305-310.

[See Superconductors.]

Steiner, B., Tseng, W.F., Comas, J., Laor, U., and Dobbyn, R.G., **Defect Formation in Semiconductor Layers During Epitaxial Growth**, Journal of Crystal Growth, Vol. 128, pp. 543-549 (August 1993).

High-resolution monochromatic synchrotron X-radiation diffraction images of several high-quality multilayer systems suggest several factors in the establishment of irregularities in layered semiconducting crystals. The nucleation of extensive arrays of dislocations during uniform 1-$\mu$m layer deposition appears to depend not only on the extent of lattice mismatch and layer thickness, but also on the regularity of the substrate. Propagation of arrays of mismatch dislocations appears to depend on the character of the unit cell.
[Contact: James Comas, (301) 975-2066]

Suehle, J.S., Cavicchi, R.E., Gaitan, M., Semancik, S., **Tin Oxide Gas Sensor Fabricated Using CMOS Micro-Hotplates and *In-Situ* Processing**, IEEE Electron Device Letters, Vol. 14, No. 3, pp. 118-120 (March 1993).

We report the first monolithic tin oxide ($SnO_2$) gas sensor realized by commercial CMOS foundry fabrication (MOSIS) and post-fabrication processing techniques. The device is composed of a sensing film that is sputter-deposited on a silicon micromachined hotplate. The fabrication technique requires no masking and utilizes *in-situ* process control and monitoring of film resistivity during film growth. Micro-hotplate temperature is controlled from ambient to 500° C with a thermal efficiency of 8° C/mW and thermal response time of 0.6 ms. Gas sensor responses of pure $SnO_2$ films to $H_2$ and $O_2$ with an operating temperature of 350° C are reported. The fabrication methodology allows integration of an array of gas sensors of various films with separate temperature control for each element in the array, and circuits for a low-cost CMOS-based gas sensor system.
[Contact: John S. Suehle, (301) 975-2247]

Plasma Processing

Recently Published

Van Brunt, R.J., and Olthoff, J.K., **Kinetic-Energy Distributions of $K^+$ in Argon and Neon in Uniform Electric Fields**, Proceedings of the 8th International Seminar on Electron and Ion Swarms, University of Trondheim, Trondheim, Norway, July 15-17, 1993, pp. 76-78.

Kinetic-energy distributions have been measured for $K^+$ ions traveling in a drift tube in argon or neon buffer gases. Measurements were made at different electric field-to-gas density ratios (E/N). The distributions were observed to deviate from a Maxwellian dependence at high E/N for neon buffer gas.
[Contact: Richard J. Van Brunt, (301) 975-2425]

Power Devices

Released for Publication

Blackburn, D.L., **Status and Trends In Power Semiconductor Devices**, to be published in the Proceedings of the IEEE Conference on Industrial Electronics (IECON '93), Maui, Hawaii, November 15-19, 1993.

A brief description of some recent developments that affect the application of power semiconductor devices is given. Developments in chips, packages, simulation, and new materials are included.
[Contact: David L. Blackburn, (301) 975-2068]

Power Devices

Recently Published

Busatto, G., Blackburn, D.L., and Berning, D.W., **Experimental Study of Reverse-Bias Failure Mechanisms in Bipolar Mode JFET (BMFET)**, Proceedings of the 1993 Power Electronics Specialists Conference, University of Seattle, Seattle, Washington, June 20-24, 1993, pp. 482-488.

A systematic, nondestructive, experimental study of the reverse-bias failure mechamisms in bipolar mode JFET behavior during its failure is presented. The variation of the reverse-bias safe-operating areas (RBSOA) for an inductive load with different bias conditions is described. It is shown that the

device breakdown is strongly dependent on the reverse current gain. On the basis of the experimental results, insight into the physics of the failure mechanisms is given, and it is shown that most of the RBSOA limitations appear to result from device lay-out problems.
[Contact: David L. Blackburn, (301) 975-2053]

Hefner, A.R., Jr., **A Dynamic Electro-Thermal Model for the IGBT**, Proceedings of the IEEE Industry Applications Society Annual Meeting, Houston, Texas, October 4-9, 1992, pp. 1094-1104.

A physics-based dynamic electro-thermal model is developed for the IGBT by coupling a temperature-dependent IGBT electrical model with dynamic thermal models for the IGBT silicon chip, packages, and heatsinks. The temperature-dependent IGBT electrical model describes the instantaneous electrical behavior in terms of the instantaneous temperature of the IGBT silicon chip surface. The instantaneous power dissipated in the IGBT is calculated using the electrical model and determines the instantaneous rate that heat is applied to the surface of the silicon chip thermal model. The thermal models determine the evolution of the temperature distribution within the thermal network, and thus determine the instantaneous value of the silicon chip surface temperature used by the electrical model. The IGBT electro-thermal model is implemented in the Saber circuit simulator and is connected to external circuits in the same way as the previously presented Saber IGBT model, except that it has an additional thermal terminal that is connected to the thermal network component models for the silicon chip, package, and heatsink. The IGBT dynamic electro-thermal model and the thermal network component models are verified for the range of temperature and power dissipation levels (heating rates) that are important for power electronic systems.
[Contact: Allen R. Hefner, Jr., (301) 975-2071]

Hefner, A.R., **Modeling Buffer Layer IGBTs for Circuit Simulation**, Proceedings of the 1993 Power Electronics Specialists Conference, University of Seattle, Seattle, Washington, June 21, 1993, pp. 60-69.

The dynamic behavior of commercially available buffer layer IGBTs is described. It is shown that buffer layer IGBTs become an order of magnitude faster at high voltages than nonbuffer layer IGBTs with similar low-voltage characteristics. Because the fall times specified in manufacturers' data sheets do not reflect the voltage dependence of switching speed, a new method of selecting devices for different circuit applications is suggested. A buffer layer IGBT model is developed and implemented into the Saber circuit simulator, and a procedure is developed to extract the model parameters for buffer layer IGBTs. It is shown that the new buffer layer IGBT model can be used to describe the dynamic behavior and power dissipation of buffer layer IGBTs in user-defined application circuits. The results of the buffer layer IGBT model are verified using commercially available IGBTs.
[Contact: Allen R. Hefner, (301) 975-2071]

Hefner, A.R., and Blackburn, D.L., **Simulating the Dynamic Electro-Thermal Behavior of Power Electronic Circuits and Systems**, Proceedings of the Third Workshop on Computers and Power Electronics, Berkeley, California, August 11, 1992, pp. 143-152 (1993).

A methodology is presented for simulating the dynamic electro-thermal behavior of power electronic circuits and systems. In the approach described, the simulator solves for temperature distribution within the semiconductor devices, packages, and heatsinks (thermal network), as well as the currents and voltages within the electrical network. The thermal network is coupled to the electrical network through the electro-thermal models for the semiconductor devices. The electro-thermal semiconductor device models calculate the electrical characteristics based upon the instantaneous value of the device silicon chip surface temperature and calculate the instantaneous power dissipated as heat within the device. The thermal network describes the flow of heat from the chip surface through the package and heatsink and, thus, determines the evolution of the chip surface temperature used by the semiconductor device models. The thermal component models for the device silicon chip, packages, and heatsinks are developed by discretizing the nonlinear heat diffusion equation and are represented in component form so that the thermal component models for various packages and heatsinks can be readily connected to one another to form the thermal

network.
[Contact: Allen R. Hefner, (301) 975-2071]

Hefner, A.R., and Blackburn, D.L., **Thermal Component Models for Electro-Thermal Network Simulation**, Proceedings of the Semiconductor Thermal Measurement and Management Symposium, Austin, Texas, February 2-4, 1993, pp. 88-96.

[See Device Physics and Modeling.]

Mantooth, H.A., and Hefner, A.R., **Electro-Thermal Simulation of an IGBT PWM Inverter**, Proceedings of the 1993 Power Electronics Specialists Conference, University of Seattle, Washington, June 21, 1993, pp. 75-84.

[See Device Physics and Modeling.]

Photodetectors

Released for Publication

Hale, P.D., and Franzen, D.L., **Accurate Characterization of High Speed Photodetectors**, to be published in the Proceedings of SPIE (The International Society for Optical Engineering, P.O. Box 10, Bellingham, Washington 98227-0010), SPIE International Symposium on Optics, Imaging, and Instrumentation, Technical Conference, San Diego, California, July 14-16, 1993.

We designed a simple heterodyne system for frequency domain characterization, intended to minimize errors due to intensity fluctuation, frequency calibration, and source impedance mismatch without using vector network analysis. A detailed uncertainty analysis for the system indicates 95 confidence intervals between ±0.25 and ±0.6 dB at 25 GHz, depending on the source impedance mismatch uncertainty.
[Contact: Paul D. Hale, (303) 497-5367]

Photodetectors

Recently Published

Gallawa, R.L., Gardner, J.L., Nettleton, D.H., and Stock, K.D., **Results of an International Intercomparison of Detector Responsivity at 1300 and 1550 nm**, Applied Optics, Vol. 31, No. 34, pp. 7226-7231 (December 1, 1992).

An international intercomparison of spectral responsivity measurements at wavelengths of interest to the optical communications community was recently completed. Thirteen countries participated in the test that was conducted in the course of a year. Results are presented. Agreement is at about the 1% level.
[Contact: Robert L. Gallawa, (303) 497-3761]

Reliability

Recently Published

Suehle, J.S., and Schafft, H.A., **Techniques and Characterization of Pulsed Electromigration at the Wafer Level**, Reliability Physics of Advanced Electron Devices, Vol. 32, No. 11, pp. 1527-1532 (November 1992). [Also published in the Proceedings of the Relectronic '91, Budapest, Hungary, August 26-30, 1991.]

Special testing techniques were developed to circumvent problems associated with high-temperature wafer-level probing and pulsed stressing of Al-Si metallizations. Recent results, using these techniques, identify new measurement interferences for highly accelerated electromigration stress tests. Measurements of the median time to failure, $t_{50}$, for dc and for pulsed current stress as a function of pulse repetition frequency reveal that highly accelerated stress tests may overestimate metallization reliability.
[Contact: John S. Suehle, (301) 975-2247]

## SIGNAL ACQUISITION, PROCESSING, AND TRANSMISSION

DC and Low-Frequency Metrology

Released for Publication

Thompson, C.A., **Apparatus for Resistance Measurement of Short, Small Diameter Conductors**.

A measurement system for determining the dc resistance of individual conductors >2 $\mu$m in diameter and 0.5 to 1 mm in length is described. The system

uses a four-probe method, computerized data acquisition and unique sample handling and contacting techniques. To demonstrate system operation, data are presented from measurements made on small-diameter copper wires. These wires were first measured in long lengths on another system and then cut into short lengths and remeasured on this system. The results from these two measurement systems are compared. From these results, we conclude that this measurement system is an effective tool for determining the resistance per unit length of short, small-diameter conductors.
[Contact: Curtis A. Thompson, (303) 497-5206]

DC and Low-Frequency

Recently Published

Avramov, S., Oldham, N.M., and Gammon, R.W., **Inductive Voltage Divider Calibration for the NASA Flight Experiment**, Proceedings of the National Conference of Standards Laboratories, Albuquerque, New Mexico, July 25-29, 1993, pp. 225-232.

The inductive voltage dividers (IVDs) used in the thermostat of NASA's Zeno experiment were tested using an automatic IVD bridge developed at the National Institute of Standards and Technology. To achieve $\pm$10-$\mu$K temperature control, the thermostat must be able to measure resistor ratios with a differential linearity $\pm$0.I parts per million. The test results show that within a ratio range of 0.5 to 0.6 at frequencies between 200 Hz and 400 Hz, the thermostat IVDs were linear to $\pm$0.07 parts per million.
[Contact: Svetlana Avramov, (301) 975-2414]

Dziuba, R.F., **Pressure Dependencies of Standard Resistors**, Proceedings of the National Conference of Standards Laboratories, Albuquerque, New Mexico, July 25-29, 1993, pp. 363-369.

The United States representation of the ohm is based on the quantized Hall resistance of 6453.20 **Ω** with a combined standard uncertainty of 0.02 parts per million. To maintain the ohm at this resistance or other resistances at this uncertainty level requires well-characterized standard resistors. A sometimes-overlooked parameter affecting standard resistors is pressure. A variety of standard resistors are examined for pressure dependencies over the range 250 hPa above and below a standard atmosphere. Results indicate that the pressure coefficients of resistance for some standards are significant.
[Contact: Ronald F. Dziuba, (301) 975-4239]

Dziuba, R.F., and Elmquist, R.E., **Improvements in Resistance Scaling at NIST Using Cryogenic Current Comparators**, IEEE Transactions on Instrumentation and Measurement, Vol. 42, No. 2, pp. 126-130 (April 1993). [Also published in the Conference Record of the Conference on Precision Electromagnetic Measurements (CPEM '92), Paris, France, June 9-12, 1992, pp. 284-285.]

Cryogenic current comparators (CCCs) are being used at NIST to verify Hamon-type resistance scaling techniques from the 1-**Ω** level to the 100-**Ω**, 1-k**Ω**, 6453.20-**Ω**, and 10-k**Ω** resistance levels. Measurements comparing the 100/1 ratio of a CCC to that of a Hamon transfer standard agree to within 0.01 parts per million - the practical limit of accuracy for a Hamon standard. The higher ratio accuracies and higher sensitivities of CCC bridges will make it possible to lower the uncertainties associated with resistance scaling at NIST by a factor of two or more.
[Contact: Ronald F. Dziuba, (301) 975-4239]

Gaitan, M., Kinard, J., and Huang, D.X., **Performance of Commercial CMOS Foundry-Compatible Multijunction Thermal Converters**, Proceedings of the Seventh International Conference on Solid-State Sensors and Actuators, Tokyo, Japan, June 7-10, 1993, pp. 1012-1014.

We report on the performance of multijunction thermal converters fabricated using commercial CMOS integrated circuit foundries through MOSIS. Calibration testing shows that the devices are suitable for the measurement of ac voltage, current, and power for frequencies above audio using conventional thermal transfer techniques. These devices show promise for applications as low-cost, high-precision rf and microwave power sensors with integrated electronics. The fabrication methodology allows easy integration with VLSI microcircuits using standard design libraries leading to low-cost, foundry-independent products.
[Contact: Michael Gaitan, (301) 975-2070]

Kinard, J.R., Lipe, T.E., and Childers, C.R., **Frequency Extension of the NIST AC-DC Difference Calibration Service for Current**, Proceedings of the 1993 National Conference of Standards Laboratories, Albuquerque, New Mexico, July 25-29, 1993, pp. 319-329.

This paper describes the NIST standards of the ac-dc difference for current and the results of a study underway to extend the frequency range down to 10 Hz and up to 100 kHz.
[Contact: Joseph R. Kinard, (301) 975-4250]

Waveform Metrology

Recently Published

Laug, O.B., Souders, T.M., and Flach, D.R., **A Custom Integrated Circuit Comparator for High Performance Sampling Applications**, IEEE Transactions on Instrumentation and Measurement, Vol. 41, No. 6, pp. 850-855 (December 1992). [Also published in the Proceedings of IEEE Instrumentation and Measurement Technology Conference, New York, New York, May 12-14, 1992, pp. 437-441.]

This paper reports on the design and performance of an application-specific integrated circuit comparator that has been optimized for equivalent-time waveform-sampling applications. The comparator, which has been fabricated with an 8.5-GHz $f_T$, bipolar silicon process, features a bandwidth of >2 GHz, a settling-time accuracy of 0.1% in 2 ns, and almost total elimination of "thermal tails" in the settling response. Several novel design features that have been used to achieve this level of performance are presented. The comparator can be used in a sampling system for both frequency domain measurements, e.g., wideband rms voltage measurements, and high-accuracy time-domain pulse measurements.
[Contact: Owen B. Laug, (301) 975-2412]

Oldham, N.M., and Hetrick, P.S., **Characterized Generator Extends Phase Meter Calibrations from 50 kHz to 20 MHz**, Conference Record of the Conference on Precision Electromagnetic Measurements (CPEM '92), Paris, France, Vol. 42, No. 2, pp. 311-313 (April 1993).

A phase angle generator made by phase locking two function generators is described. The generator produces two sine waves that are programmable in phase (0 to 360°), amplitude (0 to 40 $V_{rms}$), and frequency (1 Hz to l0 MHz). Phase linearities within $\pm 0.1^{\circ}$ are achieved without external phase standards.
[Contact: Nile M. Oldham, (301) 975-2408]

Oldham, N.M., Kramar, J.A., Hetrick, P.S., and Teague, E.C., **Electronic Limitations in Phase Meters for Heterodyne Interferometry**, Journal of the American Society for Precision Engineering, Vol. 15, No. 3, pp. 173-179 (July 1993).

Limitations imposed by the phase meters used in heterodyne interferometers are evaluated. These instruments measure the phase relationship between electrical signals generated by the heterodyning process, allowing the interferometers to resolve fractions of an optical fringe. Measurements indicate that the phase meters used in currently available heterodyne interferometers probably limit achievable accuracy to a greater extent than barriers imposed by the optics. We show that a new class of time interval counters offer a means of greatly improving accuracy in these instruments.
[Contact: Nile M. Oldham, (301) 975-2408]

Cryoelectronic Metrology

Released for Publication

Early, E.A., and Clark, A.F., **The ac Josephson Effect in Parallel Junction Arrays**.

[See Fundamental Electrical Measurements.]

Early, E.A., Steiner, R.L., Clark, A.F., and Char, K., **Evidence of Parallel Junctions Within High-$T_c$ Grain-Boundary Junctions**.

[See Fundamental Electrical Measurements.]

Goodrich, L.F., Srivastava, A.N., Stauffer, T.C., Roshko, A., and Vale, L.R., **High Current Pressure Contacts to Ag Pads on Thin Film Superconductors**.

[See Superconductors.]

Ono, R.H., Beall, J.A., Vale, L.R., and Rudman, D.A., **Transition Temperature and Orthorhombic Strain in In-situ Coevaporated $YBa_2Cu_3O_{7-\delta}$ Thin Films**.

In-situ coevaporated $YBa_2Cu_3O_{7-\delta}$ thin films have a slightly depressed transition temperature $T_c$, though they have excellent rf surface resistance characteristics. We have found that these films consistently have less orthorhombic strain than laser ablated or postannealed films. By doubling the $O_2$ partial pressure during deposition, both the $T_c$ and the orthorhombic strain were increased. Alternatively, by low-temperature (320 to 42 °C) annealing in 100 kPa of $O_2$, the $T_c$ was raised to the normal value of 91 K with a corresponding increase in the orhorhombic strain. The variation of $T_c$ with orthorhombic strain is slower for all measured thin films than for bulk material.
[Contact: Ronald H. Ono, (303) 497-3762]

Rice, J.P., **Kinetic-Inductance Infrared Detector Based on an Antenna-Coupled High-$T_c$ SQUID**, to be published in the Proceedings of the 4th International Superconductive Electronics Conference, Boulder, Colorado, Aug. 11-14, 1993.

We describe the design and estimate the performance of a high-$T_c$ kinetic-inductance infrared detector.
[Contact: Joseph P. Rice, (303) 497-7366]

Rosenthal, P.A., and Grossman, E.N., **Terahertz Shapiro Steps in High Temperature SNS Josephson Junctions**.

We have studied the far infrared behavior of high-$T_c$ superconductor-normal metal-superconductor (SNS) microbridges with $T_c$ > 85 K and critical current-resistance products ($I_cR_N$) as high as 10 mV at 4.2 K. These are the highest $I_cR_N$ products reported to date for microfabricated Josephson junctions of any material. The junctions were integrated at the feeds of planar log-periodic antennas made from Ag thin films. The junctions had dc normal state resistances $R_N$ between 6 and 38 Ω, reasonably well matched to the antenna's estimated rf impedance of 53 Ω. Far infrared laser radiation at 404-, 760-, and 992-GHz-induced distinct Shapiro steps (i.e., constant voltage steps at voltages $h(h\nu/2e)$, n=0,1,2,...) in the current voltage characteristics as well as modulation of the critical current. The amplitude of the Shapiro steps decays at voltages above 1 to 1.5 $I_cR_N$, corresponding to a maximum frequency cutoff of approximately 8 THz. These are the first far infrared measurements performed on high $T_c$ junctions. Measurements of the power, frequency, and temperature dependence of the Shapiro steps are presented and discussed in the context of a resistively and capacitively shunted junction model. A value of 4.5 fF for the junction capacitance is inferred from the hysteresis of the slightly underdamped current-voltage characteristics.
[Contact: Peter A. Rosenthal, (303) 497-7212]

Rudman, D.A., **Suitability of MOCVD-Derived $PrGaO_3$ Films as Buffer Layers for $YBa_2Cu_3O_{7-x}$ Pulsed Laser Deposition**.

Phase-pure thin films of the $YBa_2Cu_3O_{7-x}$ (YBCO) lattice-matched and low loss tangent perovskite insulator $PrGaO_3$ have been grown in situ on single-crystal (110) $LaAlO_3$ substrates (indexed in the rhombohedral system) by metal-organic chemical vapor deposition (MOCVD). Films were grown at temperatures between 750 and 800 °C using the volatile metal-organic $\beta$-diketonate precursors $M(dpm)_3$(M=Pr, Ga; dpm = dipivaloyl-methanate). YBCO films were then grown on the MOCVD-derived $PrGaO_3$ films by pulsed laser deposition (PLD). Scanning electron microscopy reveals that the MOCVD-derived $PrGaO_3$ films have smooth, featureless surfaces. As assessed by X-ray diffraction, the $PrGaO_3$ films grow epitaxially on $LaAlO_3$ with a high degree of (001) and/or (110) plane orientation parallel to the substrate surface, and the subsequent YBCO films of the trilayer grow with a high degree of c-axis orientation (00 $\ell$). Rocking curve and $\phi$-scan X-ray analyses reveal that the $PrGaO_3$ and YBCO films grow epitaxially with a high degree of crystallinity. Cross-sectional high-resolution electron microscopy and transmission electron microscopy selected-area diffraction confirm that the $PrGaO_3$ and YBCO layers grow epitaxially. YBCO films grown by PLD on the MOCVD-derived $PrGaO_3$ film exhibit a critical temperature of 91 K and a critical current density of 6 x 10 A/cm at 77 K.
[Contact: David A. Rudman, (303) 497-5081]

Cryoelectronic Metrology

Recently Published

Early, E.A., Clark, A.F., Steiner, R.L., and Char, K., **Fractional Constant Voltage Steps in Parallel Arrays of Josephson Junctions**, American Physical Society Meeting Digest, Seattle, Washington, March 22-26, 1993, p. 836.

[See Fundamental Electrical Measurements.]

Early, E.A., Steiner, R.L., Clark, A.F., and Char, K., **Half-Integral Constant Voltage Steps in Grain-Boundary High-$T_c$ Junctions**, Extended Abstracts of the Materials Research Society 1993 Spring Meeting, San Francisco, California, April 12-16, 1993, p. 388.

[See Fundamental Electrical Measurements.]

Kautz, R.L., Ono, R.H., and Reintsema, C.D., **Effect of Thermal Noise on Shapiro Steps in High $T_c$ Josephson Weak Links**, Applied Physics Letters, Vol. 61, No. 3, pp. 342-344 (July 20, 1993).

The amplitudes of Shapiro steps are measured at temperatures up to 77 K for a superconductor-normal metal-superconductor Josephson weak link fabricated from $YBa_2Cu_3O_{7-\delta}$ with a Ag-Au alloy bridge. The step amplitudes are found to be in agreement with calculations based on the resistivity shunted-junction model when the Johnson noise of the junction resistance is included.
[Contact: Richard L. Kautz, (303) 497-3391]

Missert, N., Reintsema, C.A., Beall, J.A., Harvey, T.E., Ono, R.H., Rudman, D.A., Galt, D. and Price, J.C., **Growth and Characterization of YBCO/Insulator/YBCO Trilayers**, IEEE Transactions on Applied Superconductivity, Vol. 3, No. 1, pp. 1741-1744 (March 1993).

Multilevel circuits for high-frequency applications of high-$T_c$ superconductors require low dielectric constant insulators between superconducting layers. Initial studies of $CeO_2$ thin films as the insulating layer in YBCO/insulator/YBCO structures revealed insufficient isolation between YBCO layers. Trilayer structures employing thin-film composite dielectrics of $CeO_2$ and $SrTiO_3$ were therefore investigated. Each layer grows epitaxially with a morphology comparable to that of a single YBCO film. Transport critical current density measurements of the top YBCO layer resulted in $J_c = 2 \times 10^5$ A/cm$^2$ at 77 K, a factor of 10 lower than for single films. Trilayer structures had a microwave surface resistance at 10 GHz and 4 K of 50 $\mu\Omega$, comparable to that of single films. Preliminary low-temperature measurements of the dielectric constant of composite insulator structures gave values an order of magnitude lower than for pure $SrTiO_3$.
[Contact: Carl A. Reintsema, (303) 497-5052]

Moreland, J., Harvey, T.E., Ono, R.H., and Roshko, A., **Scanned Probe Microscopy of $YBa_2Cu_3O_x$ Thin-Film Device Structures On Si Substrates**, IEEE Transactions on Applied Superconductivity, Vol. 3, No. 1, pp. 1586-1589 (March 1993).

Scanning tunneling microscopy and atomic force microscopy (AFM) have been used to image $YBa_2Cu_3O_x$ (YBCO) films grown on yttria-stabilized zirconia (YSZ) buffer layers on Si substrates. We are currently investigating the effects of deposition and patterning conditions on device topography and performance. We find evidence for pinhole formation in YSZ buffer layers and microcracking in the YBCO films. We also present AFM images of 0.25-$\mu$m-wide YBCO wires on Si made using e-beam lithography and ion milling.
[Contact: John Moreland, (303) 497-3641]

Antenna Metrology

Released for Publication

Francis, M.H., Newell, A.C., Grimm, K.R., Hoffman, J., and Schrank, H.E., **Planar Near-Field Measurements of Low-Sidelobe Antennas**, to be published in the Proceedings of the Antenna Measurement Techniques Association, Dallas, Texas, October 4-8, 1993.

The planar near-field measurement technique is a proven technology for measuring ordinary antennas operating in the microwave region. The development of very low-sidelobe antennas raised the question whether this technique could be used to accurately measure these antennas. We show that data taken with an open-ended waveguide probe and processed with the planar near-field methodolo-

gy, including probe correction, can be used to accurately measure the sidelobes of very low-sidelobe antennas to levels of -55 to -60 dB relative to the main beam peak. We discuss the major sources of error and show that the probe-antenna interaction is one of the limiting factors in making accurate measurements. The test antenna for this study was a slotted-waveguide array whose low sidelobes were known. The near-field measurements were conducted on the NIST planar near-field facility.
[Contact: Michael H. Francis, (303) 497-5873]

Francis, M.H., MacReynolds, K.M., and Canales, S., **Dual-Port Circularly Polarized Probe Standards at the National Institute of Standards and Technology**, to be published as NISTIR 5007.

Scientists at the National Institute of Standards and Technology have acquired dual-port circularly polarized probes to use as gain and near-field probe standards during the measurement of circularly polarized test antennas. These probes will serve as standards for the 18- to 26.5, 33- to 50-, and 50- to 70-GHz frequency bands. This paper discusses the need for such standards, their design requirements, the measurement results for gain, polarization, and pattern, and an error analysis of the measurement.
[Contact: Michael H. Francis, (303) 497-5873]

Guerrieri, J.R., Kremer, D.P., and Rusyn, T., **A New Extrapolation/Spherical/Cylindrical Measurement Facility at the National Institute of Standards and Technology**, to be published in the Proceedings of the 1993 Antenna Measurement Techniques Association, Dallas, Texas, October 4-8, 1993.

A new multi-purpose antenna measurement facility was put into operation at the National Institute of Standards and Technology (NIST) in 1993. This facility is currently used to perform gain, pattern, and polarization measurements on probes and standard gain horns. The facility can also provide spherical and cylindrical near-field measurements. The frequency range capability is typically from 1 to 75 GHz. This paper discusses the capabilities of this new facility in detail. The facility has 10-m-long horizontal rails for gain measurements using the NIST-developed extrapolation technique. This length was chosen so that gain calibrations at 1 GHz could be performed on antennas with apertures as large as 1 m. This facility also has a precision phi-over-theta rotator set up used to perform spherical near-field, probe pattern, and polarization measurements. This setup uses a pair of 4-m-long horizontal rails for positioning antennas over the center of rotation of the theta rotator. This allows antennas up to 2 m in length to be accommodated for probe pattern measurements. A set of 6-m-long vertical rails that are part of the source tower give the facility the added capability of performing cylindrical near-field measurements. Spherical and cylindrical near-field measurements can be performed on antennas up to 3.5 m in diameter.
[Contact: Jeffrey R. Guerrieri, (303) 497-3863]

Johnk, R.T., and Kanda, M., **An Alternative Contour Technique for the Efficient Computation of Antenna Effective Length**.

[See Radiated EMI.]

Kremer, D.P., Newell, A.C., Repjar, A.G., Rose, C., Trabelsi, A., and Pinkasi, M., **Planar Near-Field Alignment Techniques**, to be published in the Proceedings of the 1993 Antenna Measurement Techniques Association, Dallas, Texas, October 4-8, 1993.

The planarity of the scan plane used in planar near-field scanning needs to be accurately established to determine the contributions of the probe position error to the overall error budget for antenna parameter calibrations. This planarity error can be significant at millimeter-wave frequencies or for measurements of low sidelobe antennas. The National Institute of Standards and Technology has operated a planar near-field system for 20 years. During this period, scan plane characterization and alignment procedures have been developed and refined. This paper discusses one method of characterizing the scan plan for planar near-field measurements. The method uses a theodolite autocollimator, laser interferometer, electronic level, and an optical square. The data obtained using these techniques are first used to make alignment corrections to the scan plan, then new data are used to determine the best fit for the realigned scan plane. The boresight

of this plane is referenced using a permanently placed mirror. In addition, the final data obtained can be used in probe position-correction techniques, developed for planar near-field measurements.
[Contact: Douglas P. Kremer, (303) 497-3732]

Noise Metrology

Recently Published

Perera, S., **"Broadband Mismatch Error" in Noise Measurement Systems**, Conference Record of the Conference on Precision Electromagnetic Measurements (CPEM '92), Paris, France, June 9-12, 1992, pp. 256-257.

Microwave noise measurement systems of a double-sided heterodyne design, with a wide bandwidth and an electrically long transmission line at the input, may suffer from a large error; systems with a high IF are especially vulnerable. Factors contributing to this error are identified, and measures to control it are described.
[Contact: Sunchana Perera, (303) 497-3546]

Microwave and Millimeter-Wave Metrology

Released for Publication

Clague, F.R., **7-mm Coaxial Microwave Microcalorimeter**, to be published as a NIST Technical Note.

Design, evaluation, and construction details are given for the coaxial microcalorimeter used by NIST as part of the microwave power standard 7-mm coaxial transmission line. Two versions are described: one with Type N connector and one with an APC-7 connector. The operating frequency range is 0.01 to 18 GHz with either connector. The microcalorimeter is used to measure the effective efficiency of a reference standard, which is then used to calibrate other microwave power sensors. These reference standards are thermistor mounts designed by NIST to be compatible with the microcalorimeter. Detailed microcalorimeter drawings and assembly instruction are included.
[Contact: Frederick R. Clague, (303) 497-5778]

Clague, F.R., **A Method to Determine the Calorimetric Equivalence Correction for a Coaxial Microwave Microcalorimeter**, to be published in the IEEE Transactions on Instrumentation and Measurement.

This paper presents a way to obtain the microcalorimeter correction factor by direct measurement rather than by an indirect estimate or modeling. The microcalorimeter is used to measure the effective efficiency of a reference standard thermistor mount. The correction factor accounts for the different thermal paths and losses in the microcalorimeter-reference standard combination. The uncertainty in the measurement depends primarily on an accurate determination of the correction factor. This has been an especially difficult problem in the coaxial case because of the center conductor. The method requires the fabrication of components that duplicate the thermal and rf loss in the microcalorimeter and reference standard. Using the technique with the new NIST Type N coaxial microcalorimeter has substantially reduced the systematic uncertainty. The total uncertainty is about one-half the uncertainty of the prior NIST standard at frequencies above 1 GHz.
[Contact: Frederick R. Clague, (303) 497-5778]

Judish, R.M., Engen, G.F., and Juroshek, J.R., **Multi-State Two-Port: An Alternative Transfer Standard**, to be published in the Digest of the Automatic Radio Frequency Techniques Group Conference (ARFTG), Atlanta, Georgia, June 18, 1993.

The proposed use of a stable solid-state programmable impedance generator promises to simplify the operational procedures associated with calibrating vector network analyzers (VNAs). An obvious requirement for this application is that the multi-state device provide a high degree of stability and repeatability. This paper describes a series of preliminary tests which have been performed using the NIST six-port systems, and the statistical methods used to evaluate the parameters of interest. In addition, the application of this device in connector evaluation is described.
[Contact: Robert M. Judish, (303) 497-3380].

Williams, D.F., and Marks, R.B., **Accurate Trans-**

**mission Line Characterization**.

This paper introduces a new method for the characterization of transmission lines fabricated on lossy or dispersive dielectrics. The method, which is more accurate than conventional techniques, is used to examine the resistance, inductance, capacitance, and conductance per unit length of coplanar waveguide transmission lines fabricated on lossy silicon substrates.
[Contact: Dylan F. Williams, (303) 497-3138]

Microwave and Millimeter-Wave Metrology

Recently Published

Clague, F.R., **A New Coaxial Microcalorimeter Evaluation Technique**, Proceedings of the Conference on Precision Electromagnetic Measurements, Paris, France, June 9-12, 1992, pp. 387-388.

A technique for improving the evaluation of the microcalorimeter portion of a coaxial microwave power standard is described. The evaluation results in a factor that corrects for varying thermal paths and losses. This technique allows major components of the correction factor to be determined by direct measurement, rather than to be estimated indirectly.
[Contact: Frederick R. Clague, (303) 497-5778]

Jargon, J.A., and Rebuldela, G., **Measurement Service for High Power CW Wattmeters at the National Institute of Standards and Technology**, Proceedings of the Measurement Science Conference, Anaheim, California, January 21-22, 1993, unpaged.

In response to recent interest and demand for accurate high-power calibrations, the National Institute of Standards and Technology has established a measurement service for high-power continuous-wave (cw) wattmeters. The automated calibration system operates at power levels of 1 to 1000 W for frequencies from 1 to 30 MHz and 1 to 500 W for 30 to 400 MHz. The high-power source is calibrated using a transfer standard, which was calibrated using a cascaded coupler technique that is traceable to a 10-mW standard. Wattmeters are calibrated directly against the high power source and must meet the following specifications: an IEEE-488 interface bus, a type N male input connector, and either a type N female output connector or an attached load. At each measurement point the calibration factor is defined as the ratio of the wattmeter's indication to the power incident on it. Systematic uncertainties are due to the high power source calibration factors, instability of the source, resolution of the wattmeter, and reflection coefficient measurements. Random uncertainties are due to connector repeatability of the devices, environmental effects, long-term system variations, and system noise. The measurement uncertainty is less than $\pm$2% and is dependent on the frequency and power level.
[Contact: Jeffrey A. Jargon, (303) 497-3596]

Kautz, R.L., Zimmerli, G., and Martinis, J.M., **Proposed High-Accuracy Superconducting Power Meter for Millimeter Waves**, IEEE Transactions on Applied Superconductivity, Vol. 3, No. 1, pp. 2152-2155 (March 1993).

The accuracy of conventional microwave power meters is limited by the fact that some of the power dissipated in the meter is not sensed by the bolometric detector. In a proposed power meter, to be operated at 4 K, superconducting materials are used to virtually eliminate this source of error.
[Contact: Richard L. Kautz, (303) 497-3391]

Kautz, R.L., Zimmerli, G., and Martinis, J.M., **Self-Heating in the Coulomb-Blockade Electrometer**, Journal of Applied Physics, Vol. 73, No. 5, pp. 2386-2396 (March 1, 1993).

A detailed comparison between theory and experiment is used to demonstrate the presence of self-heating in the Coulomb-blockade electrometer. When three different heating models are considered, the best fit with experimental electrometer characteristics is obtained for a model in which the electron temperature of the island electrode is determined by heat transfer to the lattice via electron-phonon coupling. In the successful model, the temperature $T_i$ of the island electrons is related to the power $P_i$ dissipated in the island and the temperature $T_l$ of the phonons by $P_i = \Sigma\Omega(T_i^5 - T_l^5)$, where $\Sigma$ is an electron-phonon coupling parameter characteristic of the island material and $\Omega$ is the volume of the island. The best fit between theory

and experiment yields a value of $\Sigma = 0.2$ nW/K$^5$/$\mu$m$^3$ for the electron-phonon coupling in aluminum. Our calculations show that the electron temperature of the island commonly exceeds 100 mK even when the lattice remains at 35 mK.
[Contact: Richard L. Kautz, (303) 497-3391]

Marks, R.B., and Williams, D.F., **Traceability for On-Wafer MMIC Measurements**, Conference Record of the Conference on Precision Electromagnetic Measurements (CPEM '92), Paris, France, June 9-12, 1992, pp. 91-92.

New considerations concerning the establishment of traceability for on-wafer measurements are explored. Peculiar features related to the small size of planar transmission lines, including significant attenuation and limited reproducibility, alter our view of traceability and how it is achieved. The role of the characteristic impedance is identified, and methods for its measurement are discussed.
[Contact: Roger B. Marks, (303) 497-3037]

Wait, D.F., **A Comparison of Three Techniques for the Precision Measurement of Amplifier Noise**, Conference Record of the Conference on Precision Electromagnetic Measurements (CPEM'92), Paris, France, June 9-12, 1992, pp. 252-253.

This paper discusses three new measurement techniques and the experimental results for precision four-parameter amplifier noise measurements. Two different measurement systems were used with two different types of low-noise, X-band amplifiers. The current measurement accuracy is about ±0.2 dB.
[Contact: David F. Wait, (303) 497-3610]

Williams, D.F., and Marks, R.B., **Verification of Scattering Parameter Measurements**, Proceedings of the Conference on Precision Electromagnetic Measurements, Paris, France, June 9-12, 1992, pp. 371-372.

A powerful new technique enables the verification of the measurement accuracy of scattering parameter calibrations. This technique determines the relative impedance, the reference plane offset, and the worst-case measurement deviations of any calibration in comparison to a standard calibration. Experimental results for on-wafer measurements are presented.
[Contact: Dylan F. Williams, (303) 497-3138]

Electromagnetic Properties

Released for Publication

Baker-Jarvis, J.R., Janezic, M.D., Domich, P.D., and Geyer, R.G., **Analysis of an Open-Ended Coaxial Probe with Lift-Off for Nondestructive Testing of Dielectric and Magnetic Properties**, to be published in the IEEE Transactions on Instrumentation and Measurements.

The open-ended coaxial probe with lift-off is studied using a full-wave analysis. The field equations for the following terminations are worked out: 1) the sample is semi-infinite in extent, 2) the sample is backed by a well-characterized material, and 3) the sample is backed by a short-circuit termination. The equations are valid for both dielectric and magnetic materials. The model allows the study of the open-ended coaxial probe as a nondestructive testing tool and the analysis of the effects of air gaps on probe measurements. The reflection coefficient and phase are studied as a function of lift-off, coaxial line size, permittivity, permeability, and frequency. Numerical results compare very well to published results for the case of zero lift-off. Numerical results indicate the probe is very sensitive to lift-off. For medium to high permittivity values and electrically small probes, gaps on the order of fractions of a millimeter strongly influence the reflection coefficient. In order for the field to penetrate through the air gap, larger size coaxial line or higher frequencies need to be used. A comparison of the theory to experiment is presented. The results are in close agreement.
[Contact: James R. Baker-Jarvis, (303) 497-5621]

Grosvenor, J.H., **NIST Measurement Service for Electromagnetic Characterization of Materials**, to be published as NISTIR 5006.

This paper presents an overview of the special test/measurement services currently available at the National Institute of Standards and Technology for characterizing the dielectric and magnetic properties of materials at the rf and microwave frequencies. Many important applications of materials used

throughout the electronics, microwave, aerospace, and communications industries have created a significant and increased need for reliable data on the electromagnetic properties of such materials. This paper emphasizes recent improvements in metrology capabilities developed at NIST. These include the broadband (0.1-MHz to 18-GHz) transmission-line techniques and low-frequency parallel-plate capacitor methods. The paper also briefly addresses other facets of the NIST program, including the provision of dielectric and magnetic reference materials to customers and the organization of national round-robin intercomparisons.
[Contact: John H. Grosvenor, (303) 497-5533]

Hill, D.A., **Gradiometer Antennas for Detection of Long, Subsurface Conductors**.

The use of gradiometer antennas for detection of long conductors in tunnels is analyzed. For reception in vertical boreholes, the gradiometer consists of two vertical magnetic dipoles with a vertical separation. Both sum and difference responses are useful, but the difference response has the potential advantage of suppressing the primary field and making the scattered field easier to detect. The difference response is most effective in suppressing the primary field for a parallel scan where the transmitting antenna and receiving gradiometer are always at the same height.
[Contact: David A. Hill, (303) 497-3472]

Vanzura, E.J., Geyer, R.G., and Janezic, M.D., **The NIST 60-Millimeter Diameter Cylindrical Cavity Resonator: Performance Evaluation for Permittivity Measurements**, to be published as NIST Technical Note 1354.

Uncertainty estimates are developed for dielectric permittivity calculations made using the NIST 60-mm diameter cylindrical resonator. The cavity's cylindrical wall consists of mode-filtering helical waveguide. The cavity's length can be varied from 408 to 433 mm. Fixed-length and fixed-frequency measurements in the X-band frequency range are evaluated with particular emphasis on 10 GHz. Resonator theory and design, measurement tolerances, and software are included.
[Contact: Eric J. Vanzura, (303) 497-5752]

Vanzura, E.J., Weil, C.M., and Williams, D.F., **Complex Permittivity Measurements of Gallium-Arsenide Using a High-Precision Resonant Cavity**, Conference Record of the Conference on Precision Electromagnetic Measurements (CPEM '92), Paris, France, June 9-12, 1992, pp. 103-104.

[See Compound Materials.]

Weil, C.M., **Dielectric and Magnetic Property Measurements: The NIST Metrology Program**, to be published in the Proceedings of the Workshop on Microwave-Absorbing Materials for Accelerators, Newport News, Virginia, February 22-24, 1993.

The Electromagnetic Properties of Materials Program at the National Institute of Standards and Technology is described, including an outline of the current goals of the project as well as some details of measurement techniques being used at NIST for characterizing dielectric and magnetic materials at rf and microwave frequencies.
[Contact: Claude M. Weil, (303) 497-5305]

Electromagnetic Properties

Recently Published

Baker-Jarvis, J.R., **Dielectric and Magnetic Relaxation by Maximum-Entropy Methods**, Proceedings of the 1992 AMTA Workshop on Electromagnetic Characterization of Materials for Antenna/RCS Applications, Chicago, Illinois, July 25, 1992, pp. 1-23.

Linear and nonlinear-response theories are reviewed using classical and maximum-entropy approaches. Expressions are derived for linear and nonlinear-responses to simultaneously applied electric, magnetic, stress, and temperature fields. The statistical mechanical theories of dynamically and thermally driven systems are used to obtain new, generalized equations of evolution for the driven quantities. In a linear approximation, the Kubo expression is obtained. These equations are valid far from equilibrium. It is shown that the time evolution of the electric moment density vector can be separated into a relaxation term and an external source term. Expressions for time-dependent entropy are developed and analyzed. In the very special case of the relaxation approximation, com-

monly used in the Boltzmann equation, the equation reduces to Debye's equation. Linear constitutive relations are given for electro-acoustic interactions at low driving field strengths.
[Contact James R. Baker-Jarvis, (303) 497-5621]

Baker-Jarvis, J., Geyer, R.G., and Domich, P.D., **A Nonlinear Least-Squares Solution with Causality Constraints Applied to Transmission Line Permittivity and Permeability Determination**, IEEE Transactions on Instrumentation and Measurement, Vol. 41, No. 5, pp. 646-652 (October 1992).

A technique for the solution of 1-port and 2-port scattering equations for complex permittivity and permeability determination is presented. Using a nonlinear regression procedure, the model determines parameters for the specification of the spectral functional form of complex permittivity and permeability. The method is based on a nonlinear regression technique using the fact that a causal, analytic function can be represented by poles and zeros. The technique allows the accurate determination of many low- and high-permittivity dielectric or magnetic materials in either the low- or high-loss range. Permeability and permittivity can be obtained either from fitting all scattering-parameter data or by fitting $S_{21}$ or $S_{11}$ or $|S_{11}|$ and $|S_{21}|$ data by itself. The model allows for small adjustments, consistent with the physics of the problem, to independent variable data such as angular frequency, sample length, sample position, and cutoff wavelength. The model can determine permittivity and permeability for samples where sample length, sample position, and sample holder length are not known precisely. The problem of local minima is discussed.
[Contact: James Baker-Jarvis, (303) 497-5621]

Baker-Jarvis, J., Janezic, M.D., and Stafford, R.B., **Shielded Open-Circuited Sample Holders for Dielectric and Magnetic Measurements of Liquids and Powders**, NISTIR 5001 (March 1993).

This report overviews shielded open-circuit measurements and presents a comprehensive uncertainty analysis. We use a dominant-mode scattering formulation to develop an expression for the reflection coefficient in terms of bead and sample parameters. The formulation developed here eliminates the transformation through the various sections of the sample holder. We also extend the formulation to include magnetic measurements. The uncertainty analysis indicates a decrease in relative uncertainty with increasing sample length and with increasing frequency. The real part of the permittivity at low frequencies is very sensitive to measured phase of the reflection coefficient and sample length. The imaginary part of the permittivity of low-loss materials is not extremely sensitive to the sample length. For high-loss materials, both the real and the imaginary parts of the permittivity are sensitive to the sample lengths. The minima of the reflection coefficient for low-loss materials occur at $n\lambda_m/2$, where $n$ = 1,2,3... and $\lambda$m is the wavelength in the material. These minima in the reflection coefficient correspond to regions of minimum uncertainty for the real part of the permittivity. The minimum uncertainty for low-loss materials occurs at frequencies where there is maximal interaction of the fields with the sample.
[James R. Baker-Jarvis, (303) 497-5621]

Clark, A.V., Schaps, S.R., Baker-Jarvis, J., and Auid, B.A., **Development of Electromagnetic Probes for Intelligent Processing of Dielectric Materials**, Materials Science and Engineering Laboratory Intelligent Processing of Materials Technical Activities 1991, NISTIR 4693 (November 1991).

Electromagnetic probes are useful for characterizing the dielectric properties of materials and can be used in the intelligent processing of materials. For example, to make a homogeneous ceramic specimen with the right dielectric properties, it is necessary to have properly compacted material in the green state. Improperly compacted material can lead to the wrong complex permittivity and also to problems such as residual stress and cracking in the sintered products. It is desirable to detect improperly processed material before the "value-added" step of sintering. Another example from the electronics packaging industry is the production of printed circuit boards. Here, it is desired to have homogeneous properties; for example, no delaminations in multi-layered printed circuit boards and, also, a consistent dielectric constant. A less obvious example is foundry operations. Here, "greensand" (a mixture of sand, clay, coal and salts) is wetted with water to produce molds for

casting. Improper moisture content leads to poor quality molds and rejectable parts.

Two divisions within NIST, the Electromagnetic Fields Division and the Materials Reliability Division, are collaborating to explore the potential of electromagnetic probes for these and other practical examples. Work is proceeding to model the behavior of the probe and to perform laboratory experiments to characterize the probes and to demonstrate their practical utility.

The probes used in this research can operate with a clearance between probe and specimen (lift-off) to inspect material in a process control mode. Since these probes are sensitive to lift-off, the separation of the effects of lift-off and complex permittivity is currently being investigated theoretically.
[Contact: Alfred V. Clark, (303) 497-3159]

Optical Fiber Metrology

Released for Publication

Young, M., and Wittman, R. C., **Vector Theory of Diffraction by a Single-Mode Fiber: Application to Mode-Field Diameter Measurements**.

A vector calculation shows how to rigorously calculate the mode-field pattern of a single-mode fiber from far-field data; the result differs from scalar theory in that it predicts neither Sommerfeld's nor Kirchhoff's obliquity factor, but rather yields a result that depends on polarization.
[Contact: Matt Young, (303) 497-3223]

Optical Fiber Metrology

Recently Published

Gallawa, R.L., **Fiber Spot Size: A Simple Method of Calculation**, Journal of Lightwave Technology, Vol. 11, No. 2, pp. 192-197 (February 1993).

The ability to integrate the Laguerre Gauss functions in closed form is exploited to allow a simple but accurate evaluation of the mode field diameter of single mode fibers, building on the use of Galerkin's method. The simplicity of the method depends on the use of a pattern-matching algorithm to avoid the numerical integration normally called for. The algorithm is very fast and gives exact results. The advent of symbolic computer languages makes this approach especially easy. We used a symbolic program to predict the mode field diameter and the far-field radiation pattern and compared the results with the exact values.
[Contact: Robert L. Gallawa, (303) 497-3761]

Optical Fiber/Waveguide Sensors

Recently Published

Deeter, M.N., **High Speed, High Sensitivity Magnetic Field Sensors Based on the Faraday Effect in Iron Garnets**, Proceedings of the Ninth Optical Fiber Sensors Conference, Florence, Italy, May 3-6, 1993, pp. 409-414.

Recent research demonstrating greater performance for Faraday effect sensors based on iron garnet crystals is described. Bulk crystals are coupled to high-permeability flux concentrators, resulting in an increase in sensitivity of at least two orders of magnitude. Iron garnet films, with perpendicular magnetic anisotropy and exploited in an optical waveguide geometry exhibit greater frequency response than bulk crystals. These films also exhibit larger values of saturation Faraday rotation and ideally should exhibit no hysteresis.
[Contact: Merritt N. Deeter, (303) 497-5400]

Electro-Optic Metrology

Released for Publication

Gallawa, R.L., Kumar, A., and Goyal, I.C., **Modal Characteristics of Bent Dual-Mode Planar Optical Waveguides**.

Modal characteristics of bent dual-mode planar optical waveguides are obtained. The bending-induced changes in the modal power distribution is found to be quite different for the two modes. Surprisingly, unlike the fundamental mode, bending causes the fractional modal power for the second mode to increase in the inner core-half and to decrease in the outer core-half of the waveguide. Interestingly, this leads to a decrease in effective index of the second mode due to bending at sufficiently high V-values.
[Contact: Robert L. Gallawa, (303) 497-3761]

Gallawa, R.L., Kumar, A., and Weisshaar, A., **Fiber Splice Loss: A Simple Method of Calculation**.

We evaluate the loss encountered when splicing between two circular single-mode fibers having unmatched parameters. Our method represents a dramatic improvement in simplicity over other methods with only an insignificant degradation of accuracy. We use Galerkin's method, but expanding the field of both fibers in terms of the same set of basis functions, leading to considerable simplicity: the overlap integral is simply the inner (dot) product of the eigenvectors. Integration is thus avoided. We assume that weakly guiding conditions prevail.
[Contact: Robert L. Gallawa, (303) 497-3761]

Electro-Optic Metrology

Recently Published

Christensen, D.H., Crochiere, S.M., Pellegrino, J.G., Hill, J.R., Rai, R.S., Parsons, C.A., Hickernell, R.K., and Schaafsma, D.T., **Vertical-Cavity Semiconductor Lasers: Structural Characterization, CAD, and DFB Structures**, Proceedings of SPIE (The International Society for Optical Engineering, P.O. Box 10, Bellingham, Washington 98227-0010), OE/LASE' 93 SPIE Conference, Los Angeles, California, Vol. 1850, pp.115-121, January 18-20, 1993.

Vertical-cavity semiconductor lasers are discussed. Materials characterization methods are reviewed. Optical simulation software is discussed. Results on a novel distributed feedback laser are reported. The laser produces narrow linewidth emission compared to all reported structures to date.
[Contact: David H. Christensen, (303) 497-3354]

Gilbert, S.L., **Frequency Stabilization of a Fiber Laser to Rubidium: A High-Accuracy 1.53 $\mu$m Wavelength Standard**, Proceedings of SPIE (The International Society for Optical Engineering, P.O. Box 10, Bellingham, Washington 98227-0010), Frequency-Stabilized Lasers and Their Applications, Boston, Massachusetts, Vol. 1837, pp. 146-153, November 16-18, 1993.

Spectroscopy of the rubidium $5P_{3/2} \rightarrow 4D_{5/2}$ transition near 1.529 $\mu$m has been performed using a single-longitudinal-mode erbium-doped fiber laser. Rubidium atoms were laser-cooled and confined in a vapor-cell Zeeman optical trap. This produced a dense sample of cold atoms and reduced the Doppler broadening of the transition to less than the natural linewidth. Transition linewidths of 7 MHz were observed on the $5P_{3/2} \rightarrow 4D_{5/2}$ transition, and the fiber laser was actively stabilized to the $5P_{3/2}$, $F=3 \rightarrow 4D_{5/2}$, $F'=3$ line of $^{87}Rb$.
[Contact: Sarah L. Gilbert, (303) 497-3120]

Gilbert, S.L., **High Resolution Spectroscopy of Laser Cooled Rubidium in a Vapor Cell Trap**, Technical Digest of the Optical Society of America, Quantum Electronics and Laser Science Conference, Baltimore, Maryland, May 2-7, 1993, p. 212.

High-resolution spectroscopy has been performed using a 1.529-$\mu$m fiber laser to probe the $5P_{3/2} \rightarrow 4D_{5/2}$ transition in rubidium atoms confined in a vapor-cell trap. Line shapes and fiber laser stabilization are discussed.
[Contact: Sarah L. Gilbert, (303) 497-3120]

Patrick, H., and Gilbert, S.L., **Bragg Gratings in Optical Fibers Produced by a Continuous-Wave Ultraviolet Source**, Technical Digest of the Optical Society of America, Lasers and Electro-Optics Conference, Baltimore, Maryland, May 2-7, 1993, p. 508.

Bragg gratings with a reflectance of 50% were written in Ge-doped fiber by exposure to continuous-wave 244 nm light. The ultraviolet light was produced by frequency doubling argon-ion laser light in a buildup cavity.
[Contact: Sarah L. Gilbert, (303) 497-3120]

Complex System Testing

Released for Publication

Koffman, A.D., and Souders, T.M., **Application of the NIST Testing Strategies to a Multirange Instrument**, to be published in the Proceedings of the Measurement Science Conference, Pasadena, California, January 27-28, 1994.

A new modeling and test point reduction technique for analog and mixed-signal devices has been developed at the National Institute of Standards and Technology (NIST). This technique has been

applied as a case study to the Fluke 792A Thermal Transfer Standard for potential use in testing and calibration. An empirical model is formulated using complete test data from many devices collected from several production runs. The model is then algebraically reduced using singular value decomposition and QR decomposition. Once the final reduced model is obtained, it is used to test devices which are measured only at a reduced set of test points. The model allows accurate prediction of device behavior at all other test points. Techniques for optimal model size selection are discussed. Device modeling results are presented and compared to complete test data.
[Contact: Andrew D. Koffman, (301) 975-4518]

Complex System Testing

Recently Published

Koffman, A.D., and Stott, H.L., **Modeling and Test Point Selection for a Thermal Transfer Standard**, Proceedings of the National Conference of Standards Laboratories, Albuquerque, New Mexico, July 25-29, 1993, pp. 299-310.

Full calibration support for multirange instruments can be costly and time-consuming. This paper presents a case study in which a new empirical-model-based approach was used to substantially reduce the number of tests required to fully characterize an instrument. The Fluke 792A Thermal Transfer Standard was the subject instrument for the study. Test results showed that measurements made at 50 test points were sufficient to allow accurate predictions for the instrument's performance at all 255 test points specified by the manufacturer. An accurate model relating ac/dc difference to voltage and frequency for the instrument was formulated using complete test data from many devices collected by the manufacturer over several production runs. An empirical test point selection procedure was used to select an optimal set of test points and subsequently to predict the ac/dc differences of other 792As based on the limited set of measurements taken at the selected test points.
[Contact: Andrew D. Koffman, (301) 975-4518]

Other Signal Topics

Recently Published

Kautz, R.L., **Chaos in a Computer-Animated Pendulum**, American Journal of Physics, Vol. 61, No. 5, pp. 407-415 (May 1993).

A classroom demonstration based on computer animation illustrates chaotic motion in a driven pendulum. Generated by a 76-line program (in BASIC) that runs on PC-compatible computers, the animation shows four simultaneous displays, including the pendulum and its trajectory in state space. The program can be used to illustrate periodic attractors, symmetry breaking, period doubling, and chaos.
[Contact: Richard L. Kautz, (303) 497-3391]

## ELECTRICAL SYSTEMS

Power Systems Metrology

Released for Publication

Martzloff, F.D., **Power Quality Standards for Utilities and Their Customers**.

Power Quality issues have received increased attention in the last several years, resulting in the development of new standards addressing Power Quality concerns. This bulletin presents the background of the development of new standards on Power Quality.
[Contact: François D. Martzloff, (301) 975-2409]

Van Brunt, R.J., vonGlahn, P., and Las, T., **Nonstationary Behavior of Partial Discharge during Insulation Aging**, to be published in the Proceedings of the International Conference on Partial Discharges, London, United Kingdom, September 27-30, 1993.

The statistical properties of pulsating partial discharges (PD) generated by applying an alternating voltage to a point-dielectric gap were measured with a stochastic analyzer under conditions where the PD induced changes in the dielectric surface conductivity. The epoxy materials with and without $Al_2O_3$ filler were considered in this investigation. In the case of epoxy with filler, dramatic changes in the statistical behavior of the PD were observed to be correlated with changes in surface conductivity. These results illustrate the difficulties to be encountered in defining meaningful PD pulse "patterns"

that can be used for reliable defect site identification. An analysis of the positive and negative integrated-charge distributions also reveal problems of relating PD pulse-height data to average current measured by standard techniques.
[Contact: Richard J. Van Brunt, (301) 975-2425]

Van Brunt, R.J., vonGlahn, P., and Las, T., **Partial Discharge-Induced Aging of Cast Epoxies and Related Nonstationary Behavior of the Discharge**, to be published in the 1993 Annual Report of the IEEE Conference on Electrical Insulation and Dielectric Phenomena, New York, New York, October 17-20, 1993.

Measurements were made of the time dependences of positive and negative integrated-charge distributions for ac-generated pulsating partial discharge (PD) in point-to-dielectric gaps where the dielectric material was cast epoxy either with or without an aluminum oxide filler. Other statistical characteristics of the PD were measured such as pulse-phase distributions. The dielectric surface resistivity was measured before and after exposure to PD. For epoxy with filler, the PD statistical characteristics changed significantly during times when there was a corresponding decrease in local surface resistivity. For example, the positive PD pulses were observed to cease after a time that is inversely proportional to the frequency of the applied voltage. Partial discharge from epoxy without filler exhibited a much more stationary behavior. The connection between changes in surface resistivity and changes in stochastic behavior are explained using a Monte Carlo simulation.
[Contact: Richard J. Van Brunt, (301) 975-2425]

Power Systems Metrology

Recently Published

Misakian, M., **Coil Probe Dimension and Uncertainties During Measurements of Nonuniform ELF Magnetic Fields**, Journal of Research of the National Institute of Standards and Technology, Vol. 98, No. 3, pp. 287-295 (May-June 1993).

Comparisons are made between the average magnetic flux density as measured using single-axis and three-axis circular coil probes and the magnetic flux density at the center of the probes. The results, which are calculated assuming a dipole magnetic field, provide information on the uncertainty associated with measurements of nonuniform extremely low frequency magnetic fields produced by some electrical appliances and other electrical equipment.
[Contact: Martin Misakian, (301) 975-2426]

Sherwood, G.V., **Dimensional Characterization of Precision Coaxial Transmission Standards**, Proceedings of the 1993 Measurement Science Conference Symposium and Workshop, Anaheim, California, January 21-22, 1993, unpaged.

Precision, air-dielectric coaxial transmission line standards are commonly used with automatic network analyzers for impedance measurements. The dimensional and geometric integrity of these devices has been the subject of careful study. This report summarizes recent efforts at NIST to attain improved dimensional and geometric characterization of coaxial lines. The use of computer-aided methods that augment traditional air gaging, roundness testing, and coordinate measuring machine analysis was also discussed.
[Contact: Glenn V. Sherwood, (303) 497-3939]

Van Brunt, R.J., **Recent Developments at NIST on Optical Current Sensors and Partial Discharge Diagnostics**, Proceedings of the Electric Power Research Institute Workshop on Advanced Diagnostics for Substation Equipment, EPRI Report TR-102450, Palo Alto, California, pp. 6-159—6-173, November 3-5, 1992.

This is a summary of a presentation given at the 1992 Workshop on Advanced Diagnostics for Substation Equipment, sponsored by the Electric Power Research Institute in Palo Alto, California. Research activities at the National Institute of Standards and Technology (NIST) on development of advanced optical current sensors and partial-discharge diagnostics are briefly described. More detailed information about the research underway in these areas at NIST can be obtained from the publications cited here in the list of references. The purpose of this presentation is to draw attention to the NIST projects and discuss their relevance to the improvement of measurements applied to electric-power systems, especially those used in substations. The first activity discussed here is concerned with the use of optical fiber techniques to measure

data that should prove useful in improving the reliability of pattern recognition schemes that are under development to identify the characteristics of defect sites in the insulation at which the discharges occur.
[Contact: Richard J. Van Brunt, (301) 975-2425]

Magnetic Materials and Measurements

Released for Publication

Cross, R.W., Kos, A.B., Russek, S., Sanders, S., Parker, M., and Barnard, J., **Bulk and Local Magnetoresistance of Ni-Fe and Granular GMR Films**, to be published in the IEEE Transactions on Magnetics, Conference on Magnetism and Magnetic Materials, Minneapolis, Minnesota, November 15-18, 1993.

The magnetoresistance of Ni-Fe thin films and granular Cu/NiCoFe thin films was measured as a function of applied magnetic field magnitude and angle. The films were patterned into read-head devices with stripe widths varying from 6 to 50 $\mu$m, each having a length of 290 $\mu$m. The track width of the devices varied from 2 to 40 $\mu$m. The Ni-Fe films exhibited the well known anisotropic magnetoresistive effect, whereas the Cu/NiCoFe films exhibited the giant magnetoresistive effect (GMR). A scanning microprobe system was used to measure the local magnetoresistance in the active area of the Ni-Fe devices; the response in the central region was hysteretic and quickly saturated, whereas the response in the edge region was reversible and slow to saturate. For the GMR films, the MR response was measured as a function of decreasing device width. The response was isotropic and independent of the angle of the applied field for the bulk samples (unpatterned). For the patterned GMR devices, magnetostatic fields began to affect the magnetization distribution, causing the response to broaden. This effect was not as large as what was observed in the Ni-Fe devices. A point-source field probe was used to map the spatial sensitivity of a GMR read-head device. The probe was scanned over the plane of the device while the output voltage was monitored.
[Contact: R. William Cross, (303) 497-5300]

Rice, P., Moreland, J., and Wadas, A., **DC MFM Imaging of Thin Film Recording Heads**.

Using a new form of magnetic force microscope (DC MFM), we have made magnetic force images of a thin-film recording head. Using DC MFM, we present atomic force microscope images of the surface topography and magnetic forces taken simultaneously, allowing direct correlation of magnetic fields to the pole pieces. Magnetic force images of the head at typical head-to-disk spacings are presented. The tips used for these images had two different magnetic coatings.
[Contact: Paul S. Rice, (303) 497-3841]

Thompson, C.A., Cross, R.W., and Kos, A.B., **Micromagnetic Scanning Microprobe System**.

We describe the apparatus, instrumentation, and data acquisition techniques which make up the Micromagnetic Scanning Microprobe System (MSMS). This system was developed to study magnetoresistive (MR) thin films used in magnetic recording read heads. It uses a dc, four-probe resistance measurement technique coupled with two pairs of orthogonal field sources. Voltage contacts to the thin film are made with microprobe tips 0.1 $\mu$m in diameter on local edge and central regions of the film. Horizontal and vertical microscopes are used to verify tip placement. Results from magnetoresistance measurements of the dynamic response of a MR read head film are shown to demonstrate system operation and performance. The bulk and local magnetoresistance of a 10 $\mu$m x 10 $\mu$m NiFe thin film was measured as a function of applied field and angle. Significant variations in MR responses were seen across the width of the device because of local domain formation. The MSMS is an effective tool for characterizing the effects of domain formation on the output of a MR read head.
[Contact: Curtis A. Thompson, (303) 497-5206]

Magnetic Materials and Measurements

Recently Published

Geyer, R.G., Baker-Jarvis, J.R., Janezic, M.D., and Domich, P.D., **Spectral Characterization of Ferrites for Use as Magnetic Reference Materials**, Conference Record of the Conference on Precision Electromagnetic Measurements (CPEM

'92), Paris, France, June 9-12, 1992, pp. 107-108.

Broadband complex initial permeability and permittivity spectra of various ferrites are examined in order to assess their suitability for use as magnetic reference materials. These constant-temperature spectral measurements are made with coaxial transmission line on sintered poly-crystalline spinels and garnets of varying compositions, as well as on loaded polymers. Laboratory measurement uncertainties in both dielectric and magnetic properties are evaluated. An example of measured complex permeability and permittivity spectra of a polycrystalline Ni-Zn ferrite possessing high initial permeability with relatively low dielectric loss is given at frequencies from 300 kHz to 10 GHz. A strong single resonance behavior is apparent at frequencies between 800 MHz and 2 GHz.
[Contact: Richard G. Geyer, (303) 497-5852]

Superconductors

Released for Publication

Goodrich, L.F., Srivastava, A.N., Stauffer, T.C., Roshko, A., and Vale, L.R., **High Current Pressure Contacts to Ag Pads on Thin Film Superconductors**.

High current, low resistance, nonmagnetic, and nondestructive pressure contacts to Ag pads on $YBa_2Cu_3O_{7-\delta}$ (YBCO) thin film superconductors were obtained in this study. The contact resistance ($R_c$) reported here includes the resistance of the current lead/Ag pad interface, the Ag pad/YBCO interface, and the bulk resistance of the contact material. This total contact resistance is the relevant parameter which determines power dissipation during critical-current ($I_c$) measurements. It was found that regardless of the optimization of the Ag pad/YBCO interface through annealing, a pressure contact can yield a lower total resistance than a soldered contact. The lowest pressure contact resistance obtained was 3 $\mu\Omega$. These contacts may be useful for many different high-temperature superconductor (HTS) studies where high current contacts are needed.
[Contact: Loren F. Goodrich, (303) 497-3143]

Superconductors

Recently Published

Bray, S.L., Ekin, J.W., Kuroda, T., Wada, H., and Tsukuba-Shi, I., **Critical-Current Degradation in $NB_3Al$ Wires Due to Axial and Transverse Stress**, Fusion Engineering and Design, Vol. 20, pp. 217-275 (1993).

Effects of axial and transverse stress on the critical current of Nb-tube-processed multifilamentary Nb,Al wires have been studied. The degradations of the critical current due to axial or transverse stress for these $Nb_3Al$ wires are much smaller than those for $Nb_3Sn$ wires. The microstructures and stress states of the $Nb_3Al$ wires have been investigated to understand the stress dependences of the critical current through the microscopic observations and the elastic theory. From an engineering standpoint, the importance of mechanical strength of the matrix material where superconducting filaments are embedded has been found especially for transverse stress efforts.
[Contact: Steven L. Bray, (303) 497-5631]

Chen, D.-X., Cross, R.W., and Sanchez, A., **Effects of Critical Current Density, Equilibrium Magnetization and Surface Barrier on Magnetization of High Temperature Superconductors**, Cryogenics, Vol. 33, No. 7, pp. 695-703 (1993).

An extended critical state model which includes the effects of bulk, critical current density, equilibrium magnetization, and surface barrier is developed for the magnetization of superconductors. The equilibrium magnetization and surface barrier are modeled by an applied field-dependent surface supercurrent density $j_s(H)$, whose presence changes the boundary field of the bulk. The volume supercurrents flow with a density equal to the internal field-dependent critical current density $J_c(H_i)$. The magnetization $M$ is produced by both supercurrents. For the $M(H)$ curve computation, exponential-type $J_c(H_i)$ and $j_s(H)$ values are used for the general case of an infinite sample of rectangular cross section. A comparison between the experimental magnetization curves of a sintered $YBa_2Cu_3O_7$ superconductor at 76 K and the model fit shows that $j_s(H)$ is null for the coupling matrix, whereas a non-zero $j_s(H)$ is needed for the grains. The model fit for the irreversible magnetization of the grains is improved by including a surface barrier to the entry and exit of flux.

[Contact: R. William Cross, (303) 497-5300]

Coffey, M.W., **Nonlinear Response of Type-II Superconductors in the Mixed State in Slab Geometry**, Physical Review B, Vol. 47, No. 22, pp. 15298-15301, June 1, 1993.

The nonlinear response of a type-II superconductor of finite thickness arising from vortex motion is investigated. The results of the phenomenological theory extend the complex rf magnetic permeability and conductivity to a specific regime of nonlinear response. Explicit expressions for the complex penetration depths, amplitudes, fields, and densities for the second harmonic response with various boundary conditions are presented.
[Contact: Mark W. Coffey, (303) 497-3703]

Goldfarb, R.B., **Volume Magnetic Hysteresis Loss of $Nb_3Sn$ Superconductors as a Function of Wire Length**, Proceedings of the 8th U.S.-Japan Workshop on High-Field Superconducting Materials, Wires and Conductors, and Standard Procedures for High-Field Superconducting Wires Testing, Madison, Wisconsin, March 17-19, 1993, p. 72.

The magnetic hysteresis losses of samples of reacted multifilamentary $Nb_3Sn$ superconductor wire in coiled and straight geometries were measured at 4.1 K with a superconducting-quantum-interference-device (SQUID) magnetometer and an extraction dc magnetometer for fields perpendicular to the wire axis. There were significant differences in the volume energy dissipation for the various samples. These differences are a function only of the length of the wire samples and are independent of whether the samples are straight segments or coils. As sample length increases from 2.6 mm, losses per total sample volume, for complete field cycles of $\pm 3$ T, increase nonlinearly from 0.19 to an asymptotic value of 0.43 $MJ/m^3$. A coiled sample with wire length 3 cm has 97% of the losses of a coiled sample with wire length 15 cm or greater. Losses are very length-dependent below 1 cm.
[Contact: Ronald B. Goldfarb, (303) 497-3650]

Hyun, O.B., **Flux Expulsion at Intermediate Fields In Type-II Superconductors**, Physica C, Vol. 206, pp. 169-175 (1993).

The flux expulsion behavior at an intermediate field H ($H_{c1} << H << H_{c2}$) was studied for type-II superconductors $Nb_3Sn$, $YBa_2Cu_3O_7$, and $Bi_2Sr_2CaCu_2O_8$. Based on a temperature-dependent critical-state model, magnetization as a function of temperature M(T) for the zero-field-cooled (ZFC) measurement was used to predict flux expulsion in the field-cooled (FC) measurement and to construct the internal flux profiles for both ZFC and FC at an applied field of 1 T. The model includes empirical relations of the temperature dependence of the reversible magnetization, $M \sim (1 - t^2)$, and the critical current density, $J_c \sim (1 - t)^n$, where $t \equiv T/T_c$, at the given applied field. Various M(T) patterns are demonstrated by the exponent n, varying from 2 for $Nb_3Sn$ to over 20 for $Bi_2Sr_2CaCu_2O_8$.
[Contact: Ok-Bae Hyun, (303) 497-3725]

Roshko, A., Rudman, D.A., Vale, L.R., Goodrich, L.F., Moreland, J., and Beck, H., **Influence of Deposition Parameters on Properties of Laser Ablated $YBa_2Cu_3O_{7-\delta}$ Films**, IEEE Transactions on Applied Superconductivity, Vol. 3, No. 1, pp. 1590-1593 (March 1993).

$YBa_2Cu_3O_{7-\delta}$ films have been laser ablated under a variety of conditions, onto four different substrate materials. Using scanning tunneling microscopy, it was observed that the films grow by an island nucleation and growth mechanism. The properties of the films were studied as functions of the deposition conditions. Films on lanthanum oxide (LAO) had the best and most reproducible properties. The superconducting transition temperatures of films deposited on LAO proved to be fairly insensitive to the substrate temperature during deposition; critical transition >90 K was obtained for films deposited over a temperature range of 100 °C. The oxygen partial pressure during the deposition had a large effect on the transition temperature; the highest critical transitions were obtained for films deposited under 26.7-Pa oxygen. Measurements of transport critical current indicate that films deposited at lower temperatures are less sensitive to magnetic fields, suggesting that they may contain more defects which act as flux pinning sites.
[Contact: Alexana Roshko, (303) 497-5420]

Russek, S.E., Roshko, A., Sanders, S.C., Rudman, D.A., Ekin, J.W., and Moreland, J., **Growth of**

**Laser Ablated $YBa_2Cu_3O_{7-\delta}$ Films as Examined by RHEED and Scanning Tunneling Microscopy**, Materials Research Society 1992 Fall Proceedings, Houston, Texas, November 30-December 4, 1992, pp. 305-310.

Using scanning tunneling microscopy and reflection high-energy electron diffraction (RHEED), we have examined the growth morphology, surface structure, and surface degradation of laser-ablated $YBa_2Cu_3O_{7-\delta}$ thin films. Films from 5 nm to 1 $\mu$m thick were studied. The films were deposited on MgO and $LaAlO_3$ substrates using two different excimer laser ablation systems. Both island nucleated and spiral growth morphologies were observed depending on the substrate material and deposition rate used. The initial growth mechanism observed for a 5- to 10-nm-thick film is replicated through different growth layers up to thicknesses of 200 nm. Beyond 200 nm, the films show some a-axis grains and other outgrowths. The thinnest films (5 to 10 nm) show considerable surface roughness on the order of 3 to 4 nm. For both growth mechanisms, the ledge width remains approximately constant ($\sim$30 nm), and the surface roughness increases as the film thickness increases. The films with spiral growth have streaked RHEED patterns despite having more of a three-dimensional diffraction pattern. RHEED patterns were obtained after the film surfaces were degraded by exposure to air, KOH developer, a Br-methanol etch, and a shallow ion mill. Exposure to air and KOH developer caused only moderate degradation of the RHEED pattern, whereas a shallow (1-nm-deep) 300-V ion mill completely destroyed the RHEED pattern.
[Contact: Steven E. Russek, (303) 497-5097]

Thomson, R.E., Moreland, J., Missert, N., Rudman, D.A., and Sanders, S.C., **Observation of Insulating Nanoparticles on YBCO Thin-Films by Atomic Force Microscopy**, Proceedings of the 1993 International Workshop on Superconductivity, Hokkaido, Japan, June 28—July 1, 1993, pp. 242-243.

The surface topography of $YBa_2Cu_3O_{7-\delta}$ thin films was studied with both atomic force microscopy (AFM) and scanning tunneling microscopy (STM). The AFM images revealed a high density of small distinct nanoparticles, 10 to 50 nm across and 5 to 20 nm high, which did not appear in STM images of the same samples. Scanning the STM tip across the surface broke off the particles and moved them to the edge of the scanned area, where they were later imaged with the AFM.
[Contact: Ruth E. Thomson, (303) 497-3141]

Thomson, R.E., Moreland, J., Missert, N., Rudman, D.A., Sanders, S., and Cole, B.F., **Insulating Nanoparticles on $YBa_2Cu_3O_{7-\delta}$ Thin Films by Comparison of Atomic Force and Scanning Tunneling Microscopy**.

The surface topography of YBCO thin films has been studied with both scanning tunneling microscopy (STM) and atomic force microscopy (AFM). The AFM images reveal that these surfaces have a high density of small distinct mounds of a characteristic size (10 to 20 nm across and 5 to 10 nm high) which do not appear in STM images of the same samples. In addition, we have shown that scanning the STM tip across the surface breaks off these particles and moves them to the edge of the scanned area where they can later be imaged with the AFM.
[Contact: Ruth E. Thomson, (303) 497-3141]

## ELECTROMAGNETIC INTERFERENCE

### Radiated EMI

Released for Publication

Crawford, M.L., Riddle, B.F., and Camell, D.G., **Evaluation of TEM/Reverberating Chamber, Electromagnetic Radiation Test Facility Located at Rome Laboratory, Griffiss AFB, Rome, New York**, to be published as NISTIR 5002.

This report summarizes the measurement and evaluation of a TEM/reverberating chamber. This chamber was developed as a single, integrated facility for testing radiated electromagnetic compatibility/vulnerability (EMC/V) of large systems over the frequency range of 10 kHz to 18 GHz or higher. The facility consists of a large shielded enclosure configured as a transverse electromagnetic (TEM) transmission line-driven reverberating chamber. TEM-mode test fields are generated at frequencies below multimode cutoff, and mode-stirred test fields are generated at frequencies above multimode cutoff. The report discusses the basis for such a

development including the theoretical concepts, the advantages and limitations, the experimental approach for evaluating the operational parameters, and the procedures for using the chamber to perform EMC/V measurements. Both the chamber's cw and pulsed rf characteristics are measured and analyzed.
[Contact: Myron L. Crawford, (303) 497-5497]

Hill, D.A., **Electronic Mode Stirring for Reverberation Chambers**.

We present a model analysis and a uniform-field approximation for the fields in an idealized two-dimensional, rectangular cavity excited by an electric line source. We use the model to evaluate the effectiveness of frequency stirring, an alternative to mechanical stirring in reverberation chamber immunity measurements. Numerical results indicate that good field uniformity (standard deviation less than 1 dB) can be obtained with a bandwidth of 10 MHz at a center frequency of 4 GHz. The bandwidth requirement is determined primarily by the number of modes excited, and higher frequencies can achieve the same field uniformity with a smaller bandwidth because of the higher mode density. Cavity excitation by two single-frequency sources is also analyzed.
[Contact: David A. Hill, (303) 497-3472]

Johnk, R.T., and Kanda, M., **An Alternative Contour Technique for the Efficient Computation of Antenna Effective Length**.

The scattering problem of a plane wave broadside incident to a dipole antenna with a symmetrically placed, open-circuited gap is treated. The scattered currents on the antenna are found by solving the electric-field integral equation by means of a Galerkin moment method. The resulting current distribution is then used to compute line integrals of the scattered electric field along appropriate paths. The line integral is first evaluated directly across the dipole gap in order to compute the effective length, but severe convergence problems are encountered. This problem is due to the presence of charge singularities at the gap edges that are not accurately accounted for by the selected basis functions. Instead of attempting to incorporate the singular large behavior into the basis functions, the line integral is evaluated along an alternative contour that alleviates the convergence difficulties. This remedy is developed first for an electrostatic case and then it is applied to the dynamic scattering problem.
[Contact: Robert T. Johnk, (303) 497-3737]

Novotny, D.R., Masterson, K.D., and Kanda, M., **An Optically Linked Three-Loop Antenna System for Determining the Near-Field Radiation Characteristics of an Electrically Small Source**, to be published in the Proceedings of the 1993 IEEE International Symposium on Electromagnetic Compatibility, Dallas, Texas, August 9-13, 1993.

This paper presents the experimental results of an antenna system for determining the radiation characteristics of an electrically small source. Three orthogonal loop antennas, each terminated at diametrically opposite points with identical loads, encircle the source and characterize its equivalent electric and magnetic dipole moments. From this measurement in the near-field of the device under test, the total radiated power can be determined. The test system operates from 3 kHz to over 100 MHz with up to 90 dB of dynamic range.
[Contact: David R. Novotny, (303) 497-3168]

## Radiated EMI

Recently Published

Ma, M.T., **Selected EMC Standards and Regulations: A Summary**, NISTIR 5005 (July 1993).

This report summarizes the objective, frequency range, allowable limits, required accuracy (if any), apparatus recommended, specific parameters involved, and measurement environment for some selected regulations and standards regarding electromagnetic compatibility measurements. These regulations and standards, either enforced by the U.S. Government agencies or incorporated in voluntary industrial practice, were reviewed and critiqued in 1992. General comments are made here to each of the reviewed standards regarding the physical meaning of, and the technical factors and parameters which may affect, the measurement results. Our own competence at NIST in meeting the measurement requirements is also assessed. When appropriate, an alternative measurement

technique developed by NIST, based more on technical soundness than current practice, is offered for possible industry-wide applications.
[Contact: Mark T. Ma, (303) 497-3800].

## LAW ENFORCEMENT STANDARDS

Released for Publication

Bell, B.A., and Perrey, A.G., **NIJ Standard for Dialed Number Recorders**.

Dialed number recorders are used by local law enforcement agencies and by various federal agencies in order to prevent communication fraud, as well as other violations of federal, state, and regional laws.
[Contact: Barry A. Bell, (301) 975-2419]

## PRODUCT DATA SYSTEMS

Released for Publication

McLay, M.J., **The Role of Standards in Vacuum Electronics**, to be published in the Second Annual Vacuum Electronics Review, Department of Defense Vacuum Electronics Initiative, Alexandria, Virginia, June 29-July 1, 1993.

The spectrum of physical characteristics that are critical in vacuum electronics design makes it a particularly challenging product category to model. However, a well-integrated set of information exchange standards for vacuum electronics would provide an opportunity to reduce the cost of doing business and improve the quality of products sold. Use of existing standards and establishment of the necessary industry standards for microwave-tube design data will have significant impact on the future costs and effectiveness of maintaining and extending power-tube design systems such as Microwave and Millimeter-Wave Advanced Computational Environments (MMACE).

Cooperative development efforts such as MMACE also face broader issues of standardization. The most prominent of these are how best to exploit existing standards and what strategy to adopt when confronted with missing or conflicting standards. The MMACE approach can best be understood in terms of layered standards. At the base are common standards pertinent to a very wide variety of application areas (such as C, Portable Operating System Interface for Computer Environments (POSIX), X Windows, etc.) often sanctioned by a recognized body such as the American National Standards Institute (ANSI) or the International Standards Organization (ISO). Next come application-specific standards, such as various parts of the Standard for the Exchange of Product Model Data (STEP). Finally, there are standards and conventions formulated and used by a single company or consortium. These narrowly focused standards should be built on the underlying layers previously mentioned. The adoption of strong local standards can, moreover, provide "firewall" protection for applications even when the underlying base standards change, conflict, or simply are not there.
[Michael J. McLay, (301) 975-4099]

Parks, C., **Applying Hypertext to Managing Versions of a Standard**, to be published as NISTIR 5245.

The process of configuration management of a standard's document has traditionally been paper intensive, and has suffered from the reduction in staff-hours available to process required forms. Hypertext document files have been developed to automate this process for the Initial Graphics Exchange Specification from the raising of issues to the integration of fully approved changes. The hypertext document files take advantage of the interactive information deployment capability offered by computer databases, and the document navigation capability of hypertext. Both capabilities contribute to the quality of the standard, making the standard document and its comments visible to committee people through on-line editing and computer projection during editing. The hypertext set enables the standard to be maintained in electronic form while fulfilling all requirements for paper documented accountability and traceability records. The configuration management process includes provisions for the use of e-mail where it is available to authors and reviewers.
[Contact: Curtis H. Parks, (301) 975-3517]

Parks, C.H., and Meagher, R., **Improving the Quality of Model Reviews with Computer Hypertext Technology**, to be published in the

Proceedings of the Integrated Definition Language Users Group Fall Conference, Salt Lake City, Utah, October 18-21, 1993.

A graphic, hypertext computer application approach to facilitate the reviews of function or data models and feedback is reported. Computer modeling tools were employed, and the models transferred into hypertext for review as an alternative to the traditional manual "kit" method of documentation developed in the 1970's. This new approach has been designed and deployed to achieve consensus in the review cycle of function-decomposition modelling projects. Results are described, indicating that the benefits of employing hypertext can be realized by watching for situations appropriate to the use of hypertext in a project. Changes in the accessibility to hypertext applications, and the improvement in the ability to couple the modeling tools to hypertext model "readers" will allow a full exploration of possible benefits. This paper will describe two very different projects which use hypertext kits, one within industry, the other within an evolving standards organization.
[Contact: Curtis H. Parks, (301) 975-3517]

## VIDEO TECHNOLOGY

Bennett, H.S., Fenimore, C., Field, B.F., Kelley, E.F., **Can Displays Deliver a Full Measure?: Manufacturing**, to be published in the Proceedings of First Annual Display Manufacturing Technology Conference, San Francisco, California, January 11-13, 1994.

The National Institute of Standards and Technology (NIST) recently initiated a new program on measurements for displays. As part of this new program, NIST completed a preliminary assessment of the needs for measurements, standards, and computations to assist in the development of high-resolution displays. In this paper, we summarize the major results of this assessment and describe briefly NIST's ongoing intramural and extramural programs on displays.
[Contact: Herbert S. Bennett, (301) 975-2079]

Kelley, E.F., Field, B.F., Fenimore, C., **Nonlinear Color Transformation in Real Time Using a Video Supercomputer**, to be published in the Proceedings of the Color Imaging Conference, Phoenix, Arizona, November 7-11, 1993.

Investigations of the effects of color transformations used for video displays are often hampered by the inability to see the effects of these changes in real time for a variety of input signals. Using a video supercomputer, the Princeton Engine, the effects of a parametric nonlinear color transformation can be shown in real time.
[Contact: Edward F. Kelley, (301) 975-3842]

## ADDITIONAL INFORMATION

Lists of Publications

Smith, A.J., **Metrology for Electromagnetic Technology: A Bibliography of NIST Publications**, NISTIR 5008 (September 1993).

This bibliography lists the publications of the personnel of the Electromagnetic Technology Division of NIST during the period from January 1970 through publication of this report. A few earlier references that are directly related to the present work of the Division are also included.
[Contact: Annie Smith, (303) 497-3678]

Lyons, R.M., and Gibson, K.A., **A Bibliography of the NIST Electromagnetic Fields Division Publications**, NISTIR 5009 (September 1993).

This bibliography lists publications by the staff of the National Institute of Standards and Technology's Electromagnetic Fields Division for the period from January 1970 through July 1993. Selected earlier publications from the Division's predecessor organizations are included.
[Contact: Kathryn A. Gibson, (303) 497-3132]

Meiselman, B., **Electrical and Electronic Metrology: A Bibliography of NIST Electricity Division's Publications, NIST List of Publications 94** (January 1993).

This bibliography covers publications of the Electricity Division, Electronics and Electrical Engineering, Laboratory, NIST, and of its predecessor sections for the period January 1968 to December 1992. A brief description of the Division's technical program is given in the introduction.

[Contact: Betty Meiselman, (301) 975-2401]

Walters, E.J., **Semiconductor Measurement Technology, 1990-1992, NIST List of Publications 103** (April 1993).

The bibliography provides information on technology transfer in the field of microelectronics at NIST for the calendar years 1990 and 1992. Publications from groups specializing in semiconductor electronics are included, along with NIST-wide research now coordinated by the NIST Office of Microelectronics Programs which was established in 1991. Indices by topic area and by author are provided. Earlier reports of work performed during the period from 1962 through December 1989 are provided in NIST List of Publications 72.
[Contact: E. Jane Walters, (301) 975-2050]

Availability of *Measurements for Competitiveness in Electronics* [First Edition], NISTIR 4583 (April 1993).

This document is the successor to NISTIR 90-4260, *Emerging Technologies in Electronics ...and their Measurement Needs* [Second Edition]. The new *Measurements for Competitiveness in Electronics* identifies the measurement needs that are most critical to U.S. competitiveness, that would have the highest economic impact if met, and that are the most difficult for the broad range of individual companies to address. The document has two primary purposes: (1) to show the close relationship between U.S. measurement infrastructure and U.S. competitiveness, and show why improved measurement capability offers such high economic leverage and (2) to provide a consensus on the principal measurement needs affecting U.S. competitiveness, as the basis for an *action plan* to meet those needs and to improve U.S. competitiveness.

Copies of this document are available as Order No. PB93-160588 from the National Technical Information Service, 5285 Port Royal Road, Springfield, VA 22161, at (800) 553-6847 or (703) 487-4650.

**Abstract** -- Measurements are used to determine the values of hundreds of important quantities in the electronics industry. Representative quantities are the widths of the interconnections within semiconductor integrated circuits, the attenuation of lightwaves in optical fibers, and the signal power from microwave satellite antennas. Measurement capability is a fundamental tool used to build the nation's high-technology products. As such, it is part of the national infrastructure for the realization of these products.

Measurement capability is critical to research and development, manufacturing, marketplace entry, and after-sales support of products. Thus, measurement capability affects the performance, quality, reliability, and cost of products. The result of this pervasive impact is that the level of U.S. measurement capability places an upper limit on the competitiveness of U.S. products.

At present, U.S. industry is experiencing a major shortfall in the measurement capability needed for competitiveness in electronic products. This document identifies the measurement needs that are most critical to U.S. competitiveness, that would have the highest economic impact if met, and that are the most difficult for the broad range of individual companies to address. The measurement needs are reviewed for nine important fields of electronics, including semiconductors, magnetics, superconductors, microwaves, lasers, optical-fiber communications, optical-fiber sensors, video, and electromagnetic compatibility. These fields of electronics underlie more than $300 billion of electronic and electrical products manufactured in the U.S. each year.

This assessment provides the framework for an action plan to correct the shortfall in U.S. measurement capability in electronics and to advance U.S. competitiveness.

**Guide** -- The compiler of the document provided an introductory guide to its organization and content. Because EEEL believes that a number of *TPB* readers will be interested in the information presented in the various chapters, the contents of this guide are reproduced below (page numbers of chapter summaries are included to provide a measure of the extent of the treatment):

This document contains 12 chapters, divided into two groups. The first three chapters are introductory in nature and are relevant to all of the following chapters. The remaining nine chapters address individual fields of electronic technology. Each

chapter begins with a two-page summary that provides ready access to the major points made in the chapter. These short summaries are found on the pages identified below. By selecting from these summaries, you can quickly access information on the subjects of most interest to you.

Introductory Information -- Chapter 1, Role of Measurements in Competitiveness (page 3); Chapter 2, NIST's Role in Measurements (page 21); Chapter 3, Overview of U.S. Electronics and Electrical-Equipment Industries (page 31).

These three chapters introduce the subject of measurements and provide an overview of the products of the U.S. electronics and electrical-equipment industries.

Chapter 1, **Role of Measurements in Competitiveness**, shows why measurements are a fundamental part of the infrastructure of the nation. Chapter 1 also sets measurements in the context of the many other important factors that affect competitiveness.

Chapter 2, **NIST's Role in Measurements**, indicates the circumstances under which Government assistance to industry in the development of measurement capability is appropriate in pursuit of a strengthened national economy.

Chapter 3, **Overview of U.S. Electronics and Electrical-Equipment Industries**, introduces these industries through an overview of their major product lines. This chapter shows the various ways in which the products of these industries are commonly classified and how those classifications relate to the structure of this document.

Fields of Technology -- Chapter 4, Semiconductors (page 53); Chapter 5, Magnetics (page 95); Chapter 6, Superconductors (page 129); Chapter 7, Microwaves (page 147); Chapter 8, Lasers (page 183); Chapter 9, Optical-Fiber Communications (page ?); Chapter 10, Optical-Fiber Sensors (page ?); Chapter 11, Video (page ?); Chapter 12, Electromagnetic Compatibility (page 381)

Each of these chapters contains four basic types of information:

*Technology Review*: The field of technology is reviewed to highlight and explain the special capabilities that make the technology important. This review introduces the technical concepts that are necessary for understanding the sections that follow.

*World Markets and U.S. Competitiveness*: The economic significance of the field of technology is highlighted through use of national and international market data for major products that employ the technology. Available information on the U.S. competitiveness is described.

*Goals of U.S. Industry for Competitiveness*: The goals that U.S. industry is pursuing to improve its competitiveness are discussed so that they can be related to requirements for new measurement capability supportive of the goals.

*Measurement Needs*: The new measurement capability that U.S. industry will need to enable it to achieve its goals is described. This discussion emphasizes measurement capability that is needed widely in U.S. industry, that will have high economic impact if provided, and that is beyond the resources of the broad range of individual U.S. companies to provide.

[While the assessment of measurement needs in this document is wide ranging, not every field of technology important to the electronic and electrical-equipment industries has been covered. NIST plans to expand this assessment in future editions to include additional fields.]

The order in which chapters appear is intentional: the technologies on which most other technologies depend are introduced first. Thus, the chapter on semiconductors appears first because most electronic technologies depend on semiconductor materials. In contrast, the chapter on video is located near the end because it depends on nearly every other technology discussed earlier.

Chapters 4, 5, and 6 of this document describe the measurement needs arising from three important materials technologies that underlie current and emerging electronic and electrical products. These chapters also describe the measurement needs of components and equipment based on these materi-

als and not discussed separately in other chapters.

Chapter 4, **Semiconductors**, addresses both silicon and compound semiconductors and their use in components, including individual (discrete) electronic and optoelectronic devices and integrated circuits. Semiconductor components are central to all modern electronic products from consumer products to supercomputers.

Chapter 5, **Magnetics**, focuses on both magnetic materials and the components made from them. Magnetic materials are second in importance only to semiconductor materials for electronic products and play a central role in electrical products. This chapter also addresses the measurement needs of selected equipment critically dependent on magnetic materials, including magnetic information storage equipment, electrical power transformers, and others.

Chapter 6, **Superconductors**, examines superconductor materials and addresses both present and emerging applications of these materials in electronic and electrical products.

Chapters 7 through 11 describe the measurement needs associated with selected technologies of importance to U.S. competitiveness for current and emerging products.

Chapter 7, **Microwaves**, describes the highest-information-capacity radio technology. Microwave electronics provide the basis for modern and emerging wireless communications systems and radar systems. Included are new personal communications services with both local and worldwide access, intelligent vehicle-highway systems, and advanced audio and video broadcasting systems, among others.

Chapter 8, **Lasers**, addressed the single most important component for emerging lightwave systems used for manufacturing, medicine, communications, printing, environmental sensing, and many other applications.

Chapter 9, **Optical-Fiber Communications**, describes the highest-information-capacity cable technology. It provides the basis for national and international information highways of unprecedented performance and broad economic impact. Optical-fiber systems will be linked with microwave systems to interconnect mobile and portable users and to backup cable systems.

Chapter 10, **Optical-Fiber Sensors**, focuses on an emerging class of sensors that offers outstanding performance for a broad spectrum of applications in manufacturing, aerospace, medicine, electrical power, and other areas.

Chapter 11, **Video**, emphasizes advanced, high-performance systems, such as high-definition television, which offer, for the first time, simultaneous access to high-resolution, smooth motion, and great color depth. The chapter notes the potential of full-power implementations of video technology in interactive networked environments. The chapter contains a special focus on flat-panel displays.

Chapter 12, **Electromagnetic Compatibility**, describes the special challenges that the U.S. faces in maintaining electromagnetic compatibility among the many new products of electronic and electrical technologies. Such compatibility is essential if the full potential of all of the above technologies is to be realized without debilitating mutual interference.

Appendices -- The three appendices provide definitions of the U.S. electronics and electrical-equipment industries. These definitions were used in preparing much of the economic information in the report.

Appendix 1 describes the Standard Industrial Classification System that the U.S. Government uses for collecting data about U.S. industry. This appendix also lists publications in which the U.S. Government reports data on U.S. shipments.

Appendix 2 provides a definition of the U.S. electronics industry in terms of the Standard Industrial Classification System.

Appendix 3 provides a definition of the U.S. electrical-equipment industry in terms of the Standard Industrial Classification System.

1994 Calendar of Events

January 27, 1994 (Gaithersburg, Maryland)

**Ion Implant Users Group Meeting**. The next regularly scheduled meeting of the Ion Implant Users Group will be held at NIST in January. One of the topics scheduled for discussion is Implantation in GaAs and Other III-V Materials.
[Contact: John Albers, (301) 975-2075]

February 1-3, 1994 (San Jose, California)

**10th Annual IEEE Semiconductor Thermal Measurement and Management Symposium (SEMI-THERM)**. Sponsored by IEEE CHMT and NIST, SEMI-THERM is the premier forum for the exchange of information on thermal management of electronics systems between the academic and industrial communities. The program will address the following topics: thermal characterization; analytical and computational thermal modeling; measurement techniques including temperature, fluid flow, and thermal-mechanical properties; and thermal reliability screening and testing. SEMI-THERM has a workshop atmosphere with single-session programs coupled with technical workshops, tutorials, vendor exhibits, and optional short courses.
[Contact: David L. Blackburn, (301) 975-2053]

April 28, 1994 (Hudson, Massachusetts)

**Ion Implant Users Group Meeting**. This NIST-sponsored meeting will be held at the facilities of Digital Equipment in Hudson, Massachusetts). Among the topics to be discussed is Large Area Implantation.
[Contact: John Albers, (301) 975-2075]

June 8-10, 1994 (near Windsor, U.K.)

**IEEE/CHMT Workshop on MCM and VLSI Packaging Techniques and Manufacturing Technologies**. Sponsored by IEEE/CHMT Society and NIST, this Workshop will be held in cooperation with the European Communities DGXIII-A. The main topics of the Workshop will be the design and implementation of first-level electronic packaging and the technologies, materials, and equipment for the manufacture of multichip modules (MCM) and single-chip packages.
[Contact: George G. Harman, (301) 975-2097]

October 24-28, 1994 (Gaithersburg, Maryland)

**International Workshop on Semiconductor Materials Characterization: Present Status and Future Needs**. Papers will be presented in all relevant fields of interest to materials characterization in semiconductor device manufacturing, growth, processing, diagnostics, in-situ, real-time control and monitoring, etc. All relevant semiconductor materials will be addressed: Group IV elements, Group III-V compounds, Group II-VI compounds, IV-VI compounds, and others. The Workshop is sponsored by the Advanced Research Projects Agency (ARPA), SEMATECH, and NIST. Other co-sponsors are expected.
[Contact: David G. Seiler, (301) 975-2074]

EEEL Sponsors

National Institute of Standards and Technology
Executive Office of the President
U.S. Air Force
  Hanscom Field; Kirtland AFB; McClelland AFB; Newark Air Force Station; Space & Missile Organization; Wright-Patterson Air Force Base; SAF/FMBMB, Pentagon; Rome Labs, Griffiss AFB
U.S. Army
  Fort Belvoir; Redstone Arsenal; Fort Huachuca; Materials & Mechanics Research Strategic Defense Command
Department of Commerce
  NOAA
Department of Defense
  Advanced Research Projects Agency; Defense Nuclear Agency; Combined Army/Navy/Air Force (CCG); National Security Agency
Department of Energy
  Building Energy R&D; Energy Systems Research; Fusion Energy; Basic Energy Sciences; Oak Ridge National Lab
Department of Justice
  Law Enforcement Assistance Administration; Federal Bureau of Investigation
U.S. Navy
  Naval Sea Systems Command; Office of Naval Research; Naval Air Systems Command; Naval Air Engineering Center; Naval Surface Warfare Center; Naval Research Laboratory; Naval Command, Control and Ocean Surveillance Center; Naval Ocean Systems Center; Naval Ordnance

System Command
National Aeronautics and Space Administration
NASA Headquarters; Goddard Space Flight Center; Lewis Research Center
Nuclear Regulatory Commission
Department of Transportation
National Highway Traffic Safety Administration; Federal Aviation Administration
Tennessee Valley Authority
MIMIC Consortium
Various Federal Government Agencies

## NIST Silicon Resistivity SRMs

In response to needs of the semiconductor industry, NIST's Semiconductor Electronics Division provides silicon bulk resistivity Standard Reference Materials (SRMs) through the NIST Standard Reference Materials Program. A new class of resistivity SRMs is being introduced to respond better to users' requirements.

The first NIST (then NBS) resistivity SRMs were fabricated from crystal 50 mm (2 in) in diameter. These wafers represented various combinations of crystal growth process, crystallographic orientation, and doping, each combination chosen to give the best expected wafer uniformity for a given resistivity level. Each wafer in every set was individually measured and certified. Some of these sets are still available until the supply is exhausted (see table).

The Division is now certifying single-wafer resistivity standards at approximately the same resistivity values as were available in the earlier sets. These new SRMs are fabricated from crystal 100 mm in diameter, intended to provide improved compatibility with newer end-use instrumentation. In response to user comments, the new SRMs will be more uniform in both thickness and resistivity, will have reduced uncertainty of certified value due to use of an improved certification procedure using a four-point probe, and will be measured and certified at additional measurement sites for better characterization of wafer uniformity at its core. The additional measurements needed to qualify the improved SRMs will make them more expensive on a per-wafer basis than the earlier sets.

***NIST SILICON BULK RESISTIVITY STANDARD REFERENCE MATERIALS***

**DATE PREPARED: 8 OCTOBER 1993**

| NOMINAL RESISTIVITY (ohm · cm) | OLD SRMs | AVAILABILITY | NEW SRMs | ANTICIPATED AVAILABILITY |
|---|---|---|---|---|
| 0.01 | 1523 (one of set of two wafers) | limited supply | 2541 | to be announced |
| 0.1 | 1521 (one of set of two wafers) | limited supply | 2542 | to be announced |
| 1 | 1523 (one of set of two wafers) | limited supply | 2543 | to be announced |
| 10 | 1521 (one of set of two wafers) | limited supply | 2544 | early in calendar year 1994 |
| 25 | 1522 | set of three wafers no longer available | 2545 | to be announced |
| 75 | 1522 | | 2546 (100) | to be announced |
| 180 | 1522 | | 2547 (200) | early in calendar year 1994 |

The above table will be updated in future issues to reflect changes in availability. Every effort will be made to provide accurate statements of availability; NIST sells SRMS on an as-available basis. For technical information, contact James R. Ehrstein, (301) 975-2060; for ordering information, call the Standard Reference Materials Program Domestic Sales Office: (301) 975-6776.

# INTERNATIONAL WORKSHOP ON
# *Semiconductor Materials Characterization: Present Status and Future Needs*

## October 24-28, 1994
## Gaithersburg, Maryland, U.S.A.

## *Sponsors*

The Advanced Research Projects Agency, National Institute of Standards and Technology, and SEMATECH. Other expected co-sponsors: Air Force Office of Scientific Research, Department of Energy, Office of Naval Research, and the National Science Foundation.

## *Purpose and Goals of the Workshop*

Semiconductors form the backbone of all modern-day microelectronic and optoelectronic devices. Materials characterization has proven to be fundamental for the advancement of semiconductor technology. A comprehensive "world-class" workshop dedicated to giving critical reviews of the most important materials characterization techniques that are useful to the semiconductor industry is envisioned. Because of the increasing importance of in-line and in-situ characterization methods, a strong emphasis will be placed on ascertaining their present status and future needs.

The purpose of this workshop is to bring together scientists and engineers interested in all aspects of materials characterization (research, development, manufacturing, diagnostics...): chemical and physical, electrical, optical, in-situ, and real-time control and monitoring.

The workshop goals are: (1) to provide a forum in which measurements of current and future interest to the semiconductor industry can be reviewed, discussed, critiqued, and summarized; (2) to demonstrate and review important applications for diagnostics, manufacturing, and in-situ monitoring and control in real-time environments; and (3) to act as an important stimulus for new progress in the field by providing new perspectives.

## *Scope of the Workshop*

Papers are solicited in all relevant fields of interest to materials characterization in semiconductor device manufacturing, growth, processing, diagnostics, in-situ, real-time control and monitoring, etc. All relevant semiconductor materials will be addressed: Group IV elements (Si, etc.), Group III-V compounds (GaAs, InP, etc.), Group II-VI compounds (ZnSe, HgCdTe, etc.), IV-VI compounds (PbTe, etc.), and others. Heavy emphasis will be placed on invited papers that provide up-to-date critical reviews that discuss and evaluate the science and technology of the major techniques or areas. Recent developments of novel measurement methods will also be considered.

For technical information, contact: Dr. David G. Seiler, NIST, A305 Technology Bldg., Gaithersburg, MD 20899-0001, USA, Telephone: 301/975-2081, Fax: 301/948-4081, email: seiler@sed.eeel.nist.gov

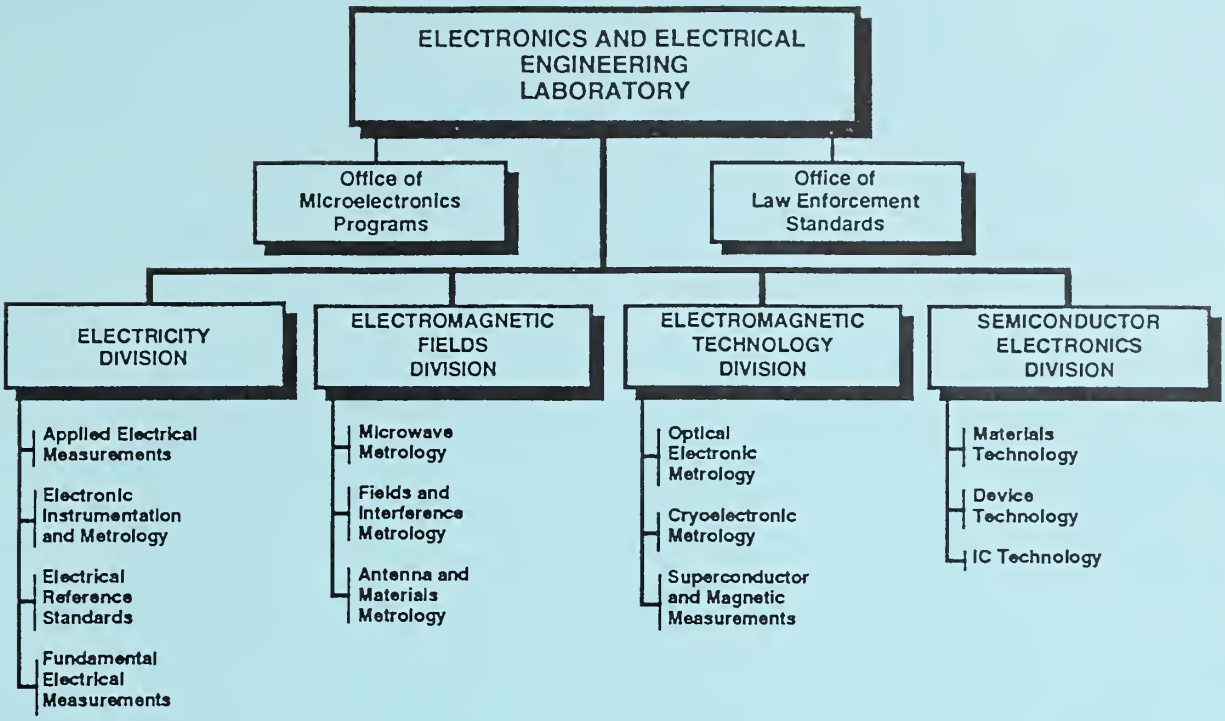


KEY CONTACTS

| | |
|---|---|
| Laboratory Headquarters (810) | Director, Mr. Judson C. French (301) 975-2220 |
| | Deputy Director, Dr. Robert E. Hebner (301) 975-2220 |
| Office of Microelectronics Programs | Director, Mr. Robert I. Scace (301) 975-2485 |
| Office of Law Enforcement Standards | Director, Mr. Lawrence K. Eliason (301) 975-2757 |
| Electricity Division (811) | Chief, Dr. Oskars Petersons (301) 975-2400 |
| Semiconductor Electronics Division (812) | Chief, Mr. Frank F. Oettinger (301)975-2054 |
| Electromagnetic Fields Divison (813) | Chief, Mr. Allen C. Newell (303) 497-3131 |
| Electromagnetic Technology Division (814) | Chief, Dr. Robert A. Kamper (303) 497-3535 |

INFORMATION:

For additional information on the Electronics and Electrical Engineering Laboratory, write or call:

Electronics and Electrical Engineering Laboratory
National Institute of Standards and Technology
Metrology Building, Room B-358
Gaithersburg, MD 20899
Telephone: (301) 975-2220

U.S. DEPARTMENT OF COMMERCE
NATIONAL INSTITUTE OF STANDARDS AND TECHNOLOGY
GAITHERSBURG, MD 20899